Paleoceanography and Paleoclimatology

RESEARCH ARTICLE
10.1029/2018PA003412

Key Points:
- North Atlantic (sub)surface temperature and seawater $\delta^{18}O$ reconstructions during the intensification of Northern Hemisphere glaciation
- Southward shifts of Subarctic Front during the intensification of Northern Hemisphere glaciation not analogous to the Last Glacial Maximum
- Dust and/or eddies are important drivers of glacial export productivity at 41°N from 2.7 Ma

Supporting Information:
- Supporting Information S1

Correspondence to:
C. T. Bolton,
bolton@cerege.fr

Citation:
Bolton, C. T., Bailey, I., Friedrich, O., Tachikawa, K., de Garidel-Thoron, T., Vidal, L., et al. (2018). North Atlantic midlatitude surface-circulation changes through the Plio-Pleistocene intensification of Northern Hemisphere glaciation. *Paleoceanography and Paleoclimatology*, *33*, 1186–1205. https://doi.org/10.1029/2018PA003412

Received 31 MAY 2018
Accepted 26 SEP 2018
Accepted article online 29 SEP 2018
Published online 9 NOV 2018

North Atlantic Midlatitude Surface-Circulation Changes Through the Plio-Pleistocene Intensification of Northern Hemisphere Glaciation

Clara T. Bolton[1], Ian Bailey[2], Oliver Friedrich[3], Kazuyo Tachikawa[1], Thibault de Garidel-Thoron[1], Laurence Vidal[1], Corinne Sonzogni[1], Gianluca Marino[4,5], Eelco J. Rohling[5], Marci M. Robinson[6], Magali Ermini[1], Mirjam Koch[7], Matthew J. Cooper[8], and Paul A. Wilson[8]

[1]Aix Marseille Université, CNRS, IRD, INRA, Coll France, CEREGE, Aix-en-Provence, France, [2]Camborne School of Mines and Environment and Sustainability Institute, University of Exeter, Penryn Campus, Cornwall, UK, [3]Institute of Earth Sciences, Heidelberg University, Heidelberg, Germany, [4]Department of Marine Geosciences and Territorial Planning, University of Vigo, Vigo, Spain, [5]Research School of Earth Sciences, The Australian National University, Canberra, Australia, [6]Eastern Geology and Paleoclimate Science Center, US Geological Survey, Reston, VA, USA, [7]Institut für Geowissenschaften, Goethe-Universität Frankfurt, Frankfurt, Germany, [8]National Oceanography Centre Southampton, University of Southampton, Southampton, UK

Abstract The North Atlantic Current (NAC) transports warm salty water to high northern latitudes, with important repercussions for ocean circulation and global climate. A southward displacement of the NAC and Subarctic Front, which separate subpolar and subtropical water masses, is widely suggested for the Last Glacial Maximum (LGM) and may have acted as a positive feedback in glacial expansion at this time. However, the role of the NAC during the intensification of Northern Hemisphere glaciation (iNHG) at ~3.5 to 2.5 Ma is less clear. Here we present new records from Integrated Ocean Drilling Program Site U1313 (41°N) spanning ~2.8–2.4 Ma to trace the influence of Subarctic Front waters above this mid-latitude site. We reconstruct surface and permanent pycnocline temperatures and seawater $\delta^{18}O$ using paired Mg/Ca-$\delta^{18}O$ measurements on the planktic foraminifers *Globigerinoides ruber* and *Globorotalia crassaformis* and determine abundances of the subpolar foraminifer *Neogloboquadrina atlantica*. We find that the first significant glacial incursions of Subarctic Front surface waters above Site U1313 did not occur until ~2.6 Ma. At no time during our study interval was (sub)surface reorganization in the midlatitude North Atlantic analogous to the LGM. Our findings suggest that LGM-like processes *sensu stricto* cannot be invoked to explain interglacial-glacial cycle amplification during iNHG. They also imply that increased glacial productivity at Site U1313 during iNHG was not only driven by southward deflections of the Subarctic Front. We suggest that nutrient injection from cold-core eddies and enhanced glacial dust delivery may have played additional roles in increasing export productivity in the midlatitude North Atlantic from 2.7 Ma.

1. Introduction

The North Atlantic Ocean is an important component of Earth's climate system because it plays a key role in the meridional heat and moisture distribution and in driving global ocean overturning circulation. Surface waters in the midlatitude North Atlantic Ocean are strongly influenced by warm and salty waters carried in by the North Atlantic Current (NAC), an extension of the Gulf Stream. The NAC flows north-eastward and is bound on its northern edge by the Subarctic (or Subpolar) Front. Together, the Subarctic Front and NAC form an oceanographic transition zone that separates cool, fresh, and nutrient-rich waters in the subpolar gyre from warmer, saltier, and relatively nutrient-depleted waters in the subtropical gyre (Krauss, 1986; Rossby, 1996). Today, the Subarctic Front is located between 45°N and 55°N in the central North Atlantic (Dickson et al., 1988). The delivery of anomalously warm and salty water to high northern latitudes via the NAC creates conditions that favor density-driven overturning and the formation of North Atlantic Deep Water, a key component of the Atlantic Meridional Overturning Circulation (Krauss, 1986; Rossby, 1996; Talley et al., 2011; Figure 1a). Changes in the position of the NAC and Subarctic Front therefore influence northern heat transport with consequences for Atlantic Meridional Overturning Circulation, high-latitude temperature, and, potentially, the growth and decay of ice sheets in the Northern Hemisphere.

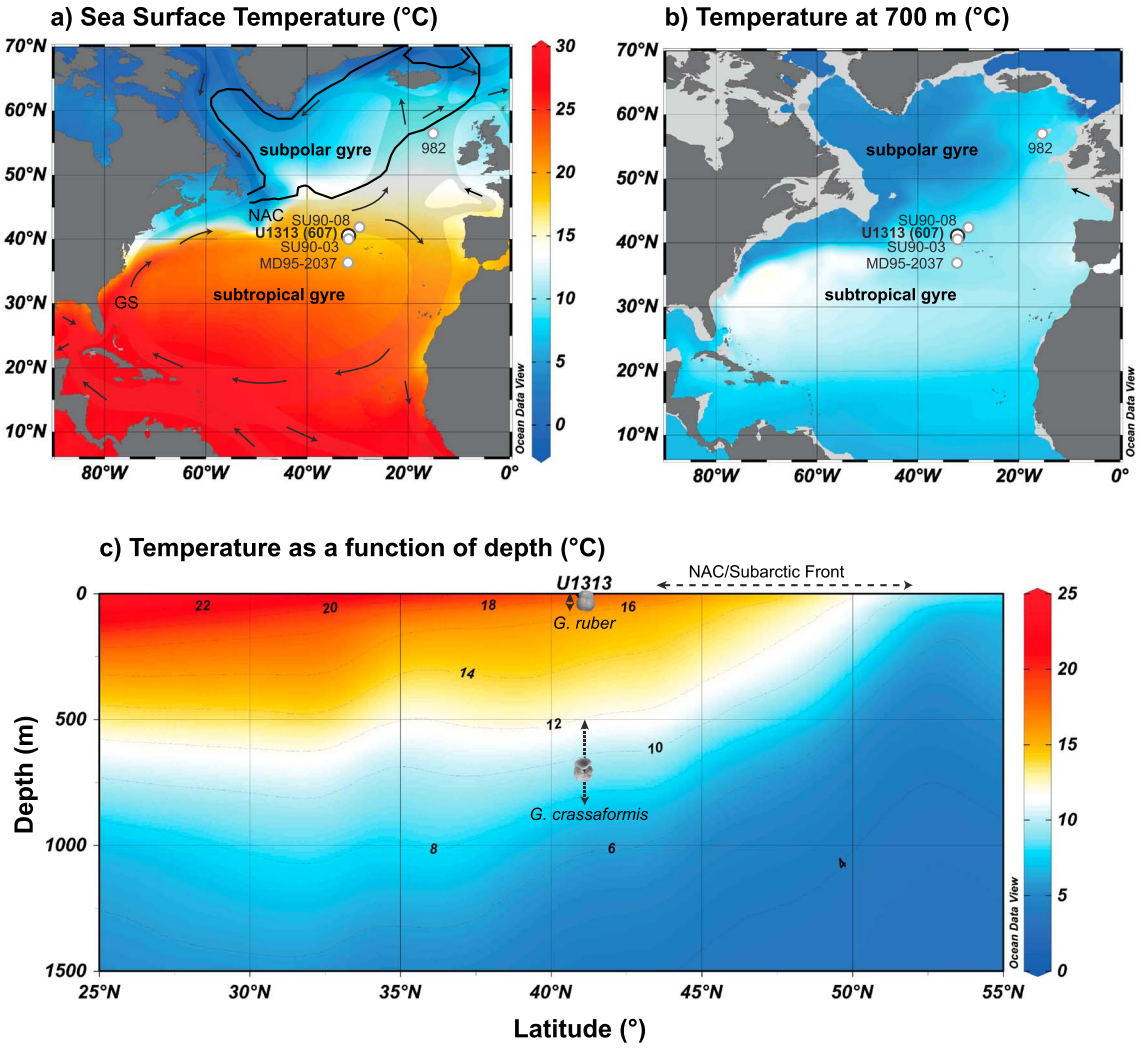

Figure 1. Modern North Atlantic temperatures and the location of Integrated Ocean Drilling Program Site U1313 and other sites discussed in the text (a) mean annual sea surface temperature and (b) mean annual temperature at 700 m depth. Black arrows show simplified surface ocean currents. GS = Gulf Stream, NAC = North Atlantic Current. Black lines show approximate front positions according to Dickson et al. (1988): PF (triangles) = Polar Front, AF (dots) = Arctic Front, SAF (dash) = Subarctic Front. (c) A north-south transect along 32.6°W (the longitude of Site U1313), showing vertical temperature structure between the surface and 1,500 m depth. The approximate depth habitats of planktic foraminiferal species studied here are shown. Maps made in Ocean Data View (Schlitzer, 2015) using World Ocean Atlas 2013 temperature data (Locarnini et al., 2013).

Based on a spatially diverse array of paleoceanographic proxy records, the Subarctic Front is suggested to have been located in the 43°N to 37°N latitude band during the Last Glacial Maximum (LGM; Bard et al., 1987; Calvo et al., 2001; Chapman et al., 2000; Chapman & Maslin, 1999; CLIMAP, 1981; Eynaud et al., 2009; Grousset et al., 1993; Pflaumann et al., 2003; Ruddiman et al., 1986, 1989; Ruddiman & McIntyre, 1976; Villanueva, Grimalt, Cortijo, et al., 1998; Waelbroeck et al., 2009). This southward displacement may have acted as an important positive feedback mechanism on glacial expansion during the last glacial cycle by amplifying cooling in high northern latitudes (Chapman & Maslin, 1999; Imbrie et al., 1992, 1993; Keffer et al., 1988; Naafs et al., 2010). The position of the Subarctic Front during the late Pliocene and earliest Pleistocene intensification of Northern Hemisphere glaciation (iNHG; 3.6–2.4 Ma; Mudelsee & Raymo, 2005) has also been studied. One interpretation of the available sea-surface temperature (SST) and productivity data for the North Atlantic is that from 2.72 Ma (marine isotope stage [MIS] G6), the glacial positioning of the NAC and Subarctic Front was comparable to that of the mid and late Pleistocene and that such changes helped to promote ice-sheet expansion in high northern latitudes (Naafs et al., 2010; Versteegh et al., 1996) and increase glacial export productivity in the midlatitude North Atlantic (Naafs et al., 2010; Versteegh et al.,

1996) from this time. This interpretation of the history of the Subarctic Front during iNHG is broadly supported by North Atlantic dinoflagellate cyst census counts, although these data sets have been used to infer a persistent influence of the NAC at ~53°N until 2.6 Ma, suggesting that the first significant southward shift of the NAC and Subarctic Front did not occur until MIS 104 (Hennissen et al., 2014). More generally, the exact magnitude of inferred southward shifts of these oceanographic fronts during iNHG glacials remains unclear. New data are therefore required to understand better the history of surface-ocean circulation reorganizations during iNHG and the potential role that they played in amplifying glacial cycles and in midlatitude export productivity increases from ~2.72 Ma. Here we address these gaps in knowledge using new surface and subsurface planktic foraminiferal records from Integrated Ocean Drilling Program (IODP) Site U1313 (41°N). Specifically, we do so by answering the following questions: (1) When did the first major southward shift of the NAC and Subarctic Front occur during iNHG? (2) Was (sub)surface reorganization in the midlatitude North Atlantic analogous to the LGM at any point during this time?

1.1. Background

Strong evidence exists for a southward shift of the Subarctic Front to between 43°N and 37°N during the LGM. In Core SU90-08 (43°N; Figure 1), sand-sized ice-rafted detritus (IRD) reached abundances of 15–30% (~500–3,000 grains/g) during background (non-Heinrich event) LGM conditions, and abundances of the polar planktic foraminifer *Neogloboquadrina pachyderma* (sinistral-coiling(s)) were ~40% (~3,000/g) (Grousset et al., 1993). A sharp gradient also existed between alkenone-based estimates of LGM SST from Core SU90-08 and Core MD95-2037 at ~37°N (10–12 and 14–15 °C, respectively). These data are interpreted to indicate a dominant influence of subpolar waters at the more northern site only (Calvo et al., 2001; Villanueva, Grimalt, Cortijo, et al., 1998). Alkenone-based SSTs above IODP Site U1313 during the LGM, which occupies a latitude intermediate to these two sites (41°N, Figure 1), were 12–13 °C (Naafs et al., 2013), and IRD and *N. pachyderma*(s) abundances were much lower than in Core SU90-08 (~50 grains/g) (Lang et al., 2016) and $<$10% (Smith et al., 2013), respectively). Higher-resolution abundance records from a site just south of Site U1313 (SU90-03, ~40°N; Figure 1) confirm that at these midlatitudes, peaks of up to 10% IRD and 15% *N. pachyderma*(s) correspond to Heinrich events, with near-zero IRD and at most 10% *N. pachyderma*(s) during ambient LGM conditions (Chapman et al., 2000). Critical to our study, these observations indicate that Sites U1313 and SU90-03 resided beneath the southern edge of the Subarctic Front *transition zone* during the LGM and beneath its northern edge only during Heinrich events (Calvo et al., 2001; Chapman et al., 2000; Eynaud et al., 2009; Lang et al., 2016; Smith et al., 2013). The warming of SSTs reported for Site U1313 during Heinrich events (Naafs et al., 2013), while not yet verified as regionally coherent (e.g., Repschläger et al., 2015), may indicate mixing of subpolar surface waters (as tracked by significant increases in *N. pachyderma*(s) abundances) with subtropical surface waters warmed by Gulf Stream pooling in the subtopics due to a reduction in Atlantic Meridional Overturning Circulation strength (Arnold et al., 2018). In the eastern North Atlantic, the Subarctic Front may have shifted south of 37°N during Heinrich events, leading to high *N. pachyderma*(s) abundances (~20–90%) in sediments deposited on the Iberian Margin (Eynaud et al., 2009) and even in the western Mediterranean Sea (Cacho et al., 1999).

In contrast to LGM studies, our understanding of the history of the NAC and Subarctic Front during iNHG is based only on paleoceanographic records from IODP Site U1313 (Deep Sea Drilling Project [DSDP] Site 607) and DSDP Site 610. On the one hand, dinoflagellate cyst concentrations in Site 607 sediments attest to increased glacial export productivity at ~41°N from 2.72 Ma (MIS G6) onward, suggested to reflect a more southerly position of the NAC and subtropical gyre boundary resulting in relatively nutrient-enriched surface waters reaching Site 607 (Versteegh et al., 1996). Alkenone data from Site U1313 corroborate this pattern, with strong glacial sea-surface cooling and higher export productivity during glacials from 2.72 Ma, similarly interpreted to show a reduced influence of the NAC and an increased influence of nutrient-rich surface waters associated with the Subarctic Front at this site (Naafs et al., 2010). The mechanism invoked by these authors to explain large productivity peaks from MIS G6 onward at 41°N, in which the *high-productivity belt* associated with the Subarctic Front migrates southward into the midlatitudes, was initially proposed for glaciations during the mid and late Pleistocene (McIntyre et al., 1972; Stein et al., 2009). On the other hand, dinoflagellate cyst assemblage data reveal large changes in surface water circulation, but only during glacials from ~2.6 Ma (MIS 104). The abundance of the NAC-indicator species *Operculodinium centrocarpum* in Site 610 sediments reveals a persistence of NAC waters above this site until MIS 104. Cold-water species only began

to dominate dinoflagellate cyst assemblages at Site 610 during this glacial, at the same time as *O. centrocarpum* first appeared in Site U1313 sediments (Hennissen et al., 2014). Based on this assemblage turnover and SST data indicating a collapse of the temperature gradient between Sites U1313 and 610, Hennissen et al. (2014) suggested that a large southward shift of the NAC and Subarctic Front first occurred during MIS 104. In addition, it remains unclear whether Subarctic Front shifts inferred for iNHG were comparable in magnitude to those reconstructed for late Pleistocene glacials. Such a strong response of North Atlantic surface circulation during MIS 104, or during any cold stage at this time, would be unexpected because global continental ice-volume during iNHG is thought to have been no more than half of that achieved during the LGM (Rohling et al., 2014).

If southward deflections of the Subarctic Front into the midlatitude North Atlantic did not occur until ~2.6 Ma, additional mechanisms must be sought to help explain the large glacial productivity peaks at Site U1313 that begin at 2.72 Ma. Indeed, during the late Pleistocene, export productivity records from the midlatitude North Atlantic appear to show a strong precessional beat evident well before the Subarctic Front is documented to have migrated to between 43°N and 37°N during the LGM (Villanueva et al., 2001). Orbitally paced productivity peaks at Sites 607 and U1313 occurring from 2.72 Ma may, for example, result from a basin-wide shoaling of the low-latitude thermocline in response to a southward shift of westerly wind belts in both hemispheres during iNHG, which would have increased the supply of (mainly southern-sourced) nutrients to the North Atlantic subtropical gyre (Lawrence et al., 2013). Since primary productivity in the region of Site U1313 today is iron-limited (Moore et al., 2006), aeolian dust deposition, which is known to have increased in the midlatitude North Atlantic during glacials from 2.72 Ma (Naafs et al., 2012), could also have played a role in stimulating glacial export productivity. Based on available data, it therefore remains unclear whether changes in surface circulation and Subarctic Front position alone can explain the temporal pattern of midlatitude productivity changes during iNHG.

Here we report a further investigation of Subarctic Front position using sediments from IODP Site U1313 spanning the interval ~2.8 to 2.4 Ma. These include high-resolution temperature and $\delta^{18}O$ recorded by two species of planktic foraminifera with surface and subsurface depth habitats and subpolar planktic foraminiferal abundances. SST data are expected to document the passage of the Subarctic Front over the core site at the surface. In addition, temperature records from deeper in the water column (500–800 m; proposed calcification depth of *G. crassaformis*) have the potential to capture southward movements of the gyre boundary even if the Subarctic Front was located consistently north of the study site at the surface, because the anatomy of the gyre is such that the boundary between subtropical and subpolar waters occurs further south at this depth relative to its position at the surface (Figure 1c). The abundance of the polar planktic foraminifera *N. pachyderma*(s) is a powerful tool to track the position of the Subarctic Front during the last glacial cycle (Chapman et al., 2000; Eynaud et al., 2009; Grousset et al., 1993; Pflaumann et al., 2003; Smith et al., 2013; Figures 2a and 2b). During the mid to late Pliocene, *N. atlantica* had a similar subpolar distribution in the North Atlantic, with abundances of 20–70% during iNHG glacials at sites between 48°N and 56°N (Berggren, 1972; Dowsett et al., 2015; Dowsett & Poore, 1990; Dowsett & Robinson, 2007; Loubere, 1988; Loubere & Moss, 1986; Poore & Berggren, 1975; Raymo et al., 1986; Robinson, 2018). Although most detailed reconstructions are from the PRISM interval (3.39–2.97 Ma; Figures 2c and 2d), a similar picture can be gleaned from foraminiferal data spanning all of iNHG (Loubere, 1988; *Loubere & Moss,* 1986; Raymo et al., 1986). We therefore use *N. atlantica* abundances as an additional tracer of subpolar waters.

2. Materials and Methods

2.1. Drill Site and Sampling

IODP Site U1313 (41°N, 32.5°W, water depth 3,426 m), located beneath the northern part of the subtropical gyre in the modern North Atlantic Ocean (Figure 1), is a reoccupation of benchmark site DSDP Site 607 that benefits from modern drilling and splicing techniques and excellent recovery (Shipboard Scientific Party, 2006). Proxy records generated from Site 607 and U1313 sediments have provided important insight into North Atlantic climate evolution during iNHG (Becker et al., 2006; Bolton et al., 2010; Friedrich et al., 2013; Hennissen et al., 2014; Lang et al., 2014, 2016; Lawrence et al., 2009, 2013; Naafs et al., 2010, 2012; Raymo et al., 1989, 1990, 1992, 2004; Ruddiman et al., 1989; Versteegh et al., 1996). Our samples come from the primary shipboard splice and have a depth spacing of 2 cm for the interval deposited during MIS

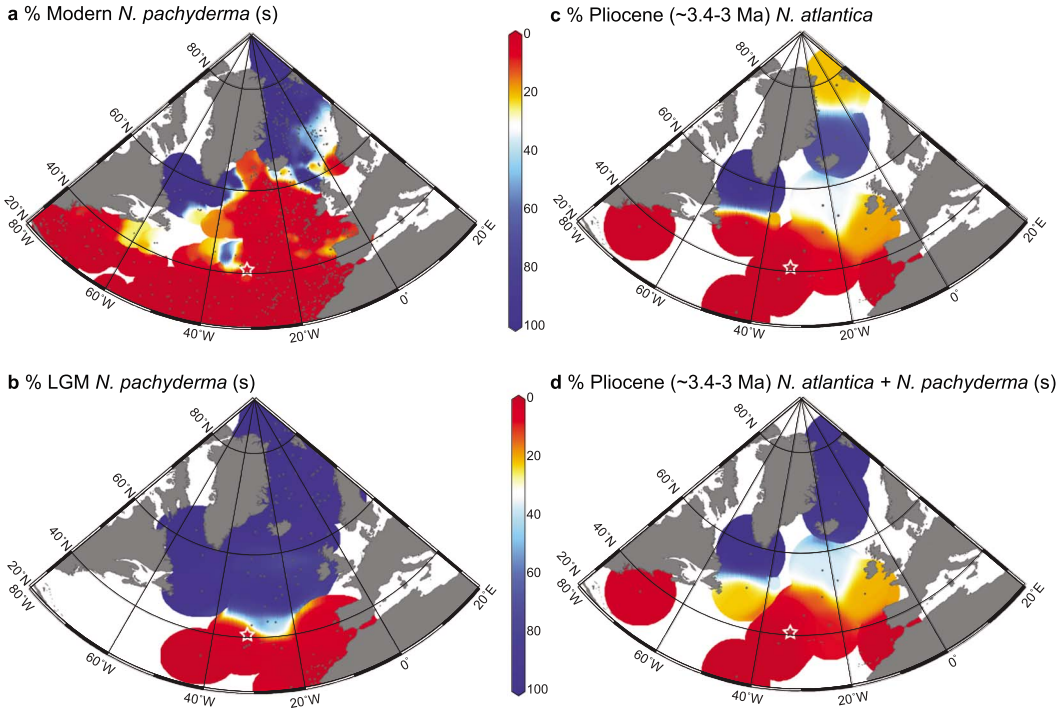

Figure 2. Modern and past distribution of the relative abundance of polar/subpolar planktic foraminiferal species in the North Atlantic. (a) Percent *N. pachyderma*(s) in North Atlantic core-top samples (data compiled in Waelbroeck et al., 2009), (b) percent *N. pachyderma*(s) in sediments deposited during the Last Glacial Maximum (LGM; Waelbroeck et al., 2009), (c) percent *N. atlantica* in sediments deposited during the warm Pliocene PRISM time slab (3.39–2.97 Ma), and (d) the sum of *N. atlantica* and *N. pachyderma*(s) abundances deposited in sediments during the PRISM time slab. All Pliocene data are from Dowsett et al. (2015) and Foley et al. (2015), except those from Deep Sea Drilling Project Site 548 (Loubere & Moss, 1986; PRISM Project Members, 1996) and from Nordic Sea sites ODP 907 and 909 (Robinson, 2018). Average abundances plotted for Nordic Sea ODP Sites 907 and 909 represent percentages when Nordic Sea surface waters were warm enough to support foraminifera. *Neogloboquadrina atlantica* relative abundances at very high northern latitudes (ODP Site 909) are lower than at subpolar latitudes because *N. pachyderma*(s) dominated these very cold waters during the Pliocene (compare panels (c) and (d)). Gray dots show sites used in the gridded data compilations. White star shows the location of Integrated Ocean Drilling Program Site U1313. Maps made using Ocean Data View (Schlitzer, 2015).

103 to 95 (122.74 to 114.50 m composite depth, mcd) and 5 cm from sediments deposited during MIS G11 to MIS 104 (133.76 to 122.74 m composite depth). Sediments in our study interval are carbonate-rich, alternating nannofossil ooze, silty clay nannofossil ooze, and nannofossil ooze with clay (Shipboard Scientific Party, 2006). We apply the age model of Bolton et al. (2010), which is based on tuning of the Site U1313 benthic $\delta^{18}O$ record to the global LR04 stack (Lisiecki & Raymo, 2005). This yields an average temporal resolution of 0.4 and 1.2 ky in the younger and older parts of the record, respectively.

2.2. Water Column Structure, Seasonality, and Depth Habitats

In the North Atlantic subtropical gyre, the surface mixed layer overlies the seasonal (absent in winter) pycnocline. Below this, surface mode waters sit on top of the permanent pycnocline, which represents the transitional layer between overlying mode waters and underlying deeper water masses (Feucher et al., 2016; Sprintall & Cronin, 2001; Talley et al., 2011). The depth, thickness, and amplitude (gradient strength) of stratification of the permanent pycnocline vary spatially across the subtropical gyre. Its estimated depth above Site U1313 is between 700 and 750 m, with a total pycnocline thickness of 350–400 m (Feucher et al., 2016). Modern, seasonal SST variability above Site U1313 is ~3.8 °C (Locarnini et al., 2013). We studied two species of planktic foraminifera with different depth habitats to reconstruct ocean conditions in the surface mixed layer (*Globigerinoides ruber*) and in the permanent pycnocline (*Globorotalia crassaformis*) using geochemical proxies.

Globigerinoides ruber is a warm-water tropical to subtropical species, known to live and calcify in the surface mixed layer of the ocean at temperatures between 13 and 32 °C (Bijma et al., 1990; Schmidt & Mulitza, 2002; Tolderlund & Bé, 1971) and depths of 0–50 m (Anand et al., 2003). *Globigerinoides ruber* sensu stricto, selected for this study, is thought to have a shallower calcification depth (0–30 m) relative to other morphotypes within the broader *G. ruber* (Aurahs et al., 2011; Kuroyanagi & Kawahata, 2004; Regoli et al., 2015; L Wang, 2000). In the eastern North Atlantic Ocean today, peak abundances of *G. ruber* are recorded during August (Schiebel & Hemleben, 2000). Thus, temperatures derived from *G. ruber* at Site U1313 likely represent late summer temperatures above the seasonal pycnocline (Friedrich et al., 2013; Robinson et al., 2008).

Globorotalia crassaformis is a geographically widespread species in the tropical and subtropical oceans. Plankton samples from the tropical Indian and Atlantic Oceans suggest a preference for cool subsurface waters (~18 ± 3.8 °C and 50–500-m water depth; Bé & Hutson, 1977; Jones, 1967; Kemle-von Mücke & Oberhänsli, 1999). Calcification depth estimates for *G. crassaformis* in the (sub)tropical Atlantic Ocean, based on modern hydrographic data combined with foraminiferal oxygen isotope ratios ($\delta^{18}O$) measured in core-tops (Steph et al., 2009) or sediment traps (Anand et al., 2003), are between 500 and 800 m. A study of $\delta^{18}O$ and Mg/Ca in *G. crassaformis* tests deposited across a latitudinal transect of the Atlantic Ocean (25°S to 45°N) suggests a mean calcification depth of 700 m, with greater calcification depths in the central subtropical gyre regions that shoal toward the subpolar regions and the equator (Cléroux et al., 2013). Thus, *G. crassaformis* consistently calcifies within the depth range of the permanent pycnocline in the N. Atlantic subtropical gyre (Cléroux et al., 2013; Feucher et al., 2016). This species' geochemical signature is not thought to carry a seasonal bias because conditions in the depth range of *G. crassaformis* are relatively constant on seasonal timescales (e.g., Tedesco et al., 2007).

2.3. Planktic Foraminiferal Proxies

High-resolution records of *G. ruber* $\delta^{18}O$ and Mg/Ca from Site U1313 for the interval MIS 103 to 95 (~2600–2400 ka) are published in Bolton et al. (2010) and Friedrich et al. (2013), respectively. Here we extend these records back to MIS G11 (~2830 ka). We also present new records of $\delta^{18}O$ and Mg/Ca from *G. crassaformis* and an *N. atlantica* abundance record spanning MIS G11 to 95. Samples were washed over a 63-μm sieve and oven dried at 50 °C. Sixty to seventy individuals of *G. ruber* (sensu stricto) and 30–40 individuals of *G. crassaformis* were picked for paired stable isotope-trace element analyses. *G. ruber* were picked from the 212–250 μm fraction and *G. crassaformis* from the 315–355 μm fraction, thus minimizing intraspecific size effects on $\delta^{18}O$ and Mg/Ca ratios (Ezard et al., 2015; Friedrich et al., 2012). Foraminifera in each sample were individually cracked using a needle under the binocular microscope to break open all chambers. Test fragments were thoroughly mixed and split for Mg/Ca (two thirds) and $\delta^{18}O$ (one third) analyses on the same fossil populations.

Samples for Mg/Ca were cleaned following the protocol described in Barker et al. (2003). After cleaning, samples were dissolved in 500 μl of 0.075 M HNO_3^- and centrifuged to ensure removal of any detrital particles. The upper 450 μl of the centrifuged solution was then transferred to a clean tube. Sample solutions were analyzed on a Perkin Elmer Optima 4300DV inductively coupled plasma-optical emission spectrometer (ICP-OES) at the National Oceanography Centre Southampton (NOCS) or a Jobin Yvon Ultima C ICP-OES at CEREGE. The accuracy of Mg/Ca measurements at NOCS and CEREGE was confirmed by international calibration studies (Greaves et al., 2008; Rosenthal et al., 2004). House standard solutions were analyzed every five samples during the sequences. The estimated typical precision was better than 0.5% (Green et al., 2003; Tachikawa et al., 2014). $\delta^{18}O$ measurements were performed on a Thermo Scientific MAT-253 mass spectrometer coupled to a Gasbench II at Goethe University Frankfurt or a Finnigan Delta Advantage mass spectrometer coupled to a Kiel device at CEREGE. All values are reported relative to the Vienna Pee Dee Belemnite standard. Analytical precision ($\pm 1\sigma$) was better than 0.08‰ (Frankfurt) and 0.05‰ (CEREGE), based on repeat analysis of the NBS-19 limestone standard. For Mg/Ca and $\delta^{18}O$ and for both species, replicate analyses from a subset of samples were prepared and measured in the two laboratories, confirming that there were no instrument offsets (Figure 3, see caption for details).

Abundances of the planktic foraminifer *N. atlantica* were counted in statistically representative splits of the >150-μm sample fraction containing at least 300 whole planktic foraminifera. Samples were counted at 20 cm sample spacing from MIS G11 to 95, and at 2 to 5 cm spacing in intervals where the species was

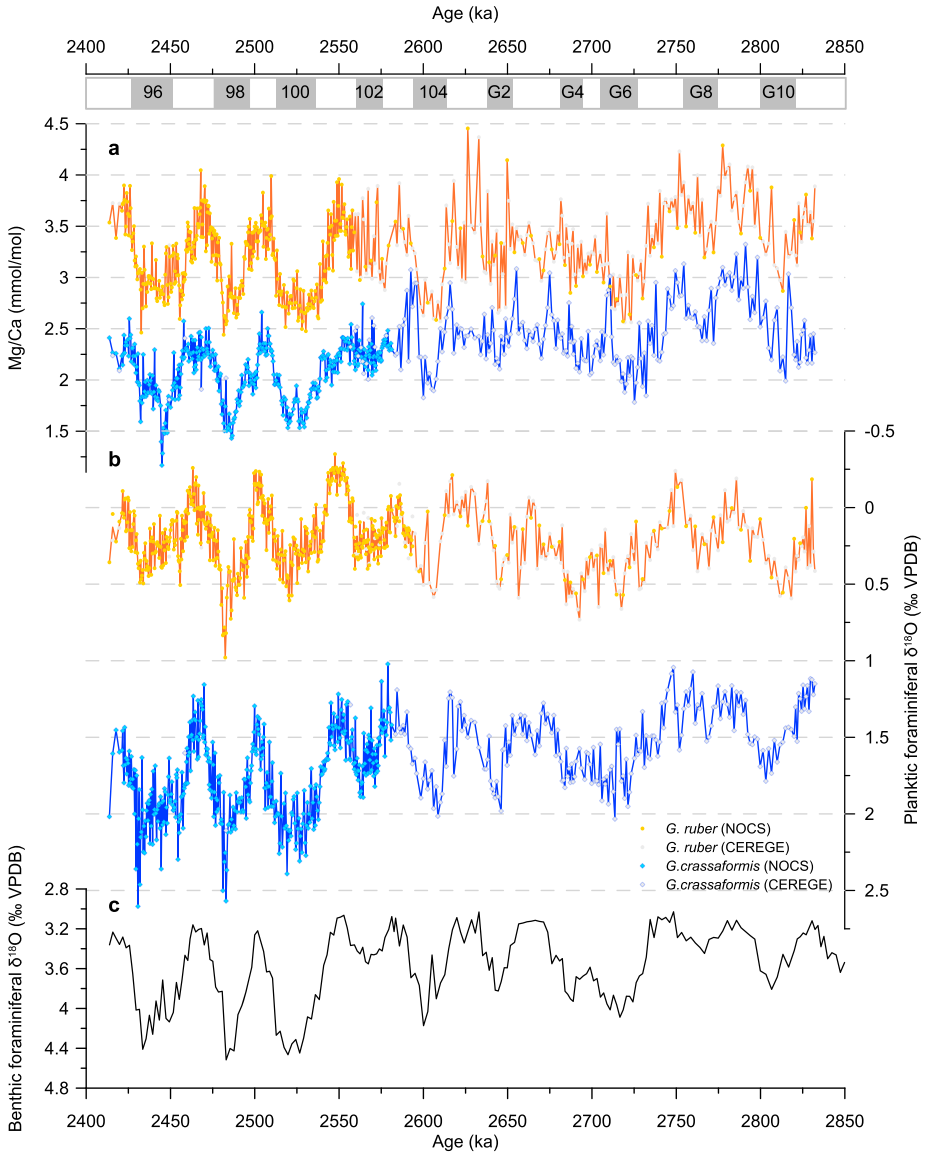

Figure 3. (a) Mg/Ca and (b) $\delta^{18}O$ in *G. ruber* (orange) and *G. crassaformis* (blue) from Site U1313. (c) Site U1313 *Cibicidoides wuellerstorfi* benthic foraminiferal $\delta^{18}O$ record (picked from the same samples, corrected to equilibrium by adding +0.64‰), originally published in Bolton et al. (2010). In (a) and (b), symbol fill color indicates the laboratory in which samples were analyzed (see legend). For *G. crassaformis* and *G. ruber*, 20 samples were picked, cleaned, and analyzed independently for Mg/Ca at NOCS and CEREGE, confirming that there were no interlab offsets. In particular, we analyzed 14 *G. crassaformis* samples during marine isotope stages (MIS) 101 to 103 in both labs to verify that the step change in Mg/Ca at this time was a real feature of the record. Furthermore, the existence of a lower resolution (20 cm) *G. ruber* Mg/Ca record spanning MIS G11 to 103 generated at NOCS (Friedrich et al., 2013) allows us to confirm good agreement with the new higher-resolution data generated at CEREGE. High-resolution *G. ruber* data spanning MIS 103–95 are originally published in Bolton et al. (2010) and Friedrich et al. (2013). Glacial MIS numbers are indicated. VPDB = Vienna Pee Dee Belemnite.

present. Abundances are expressed both as percent relative to total planktic foraminifera and also as numbers per gram of dry bulk sediment to eliminate potential closed-sum effects.

2.4. Temperature and $\delta^{18}O$ Residual Calculations

To convert Mg/Ca ratios in *G. ruber* (white) into seawater temperature (*T*), we used a species-specific calibration based on Atlantic sediment trap samples: $T = (1/0.09) \times \ln(Mg/Ca/0.449)$ (Anand et al., 2003; see Friedrich et al., 2013, for a detailed discussion of the choice of *G. ruber* calibration at Site U1313). A

few Mg/Ca-*T* calibrations exist for *G. crassaformis*. One is based on Atlantic core-top data (Cléroux et al., 2013). However, because that study included a reductive step in the Mg/Ca cleaning protocol, with potential implications for Mg/Ca ratios, we applied the calibration of Regenberg et al. (2009), for which the Mg/Ca cleaning protocol used is identical to that in our study. We used the *deep-thermocline species* equation of Regenberg et al. (2009): $T = (1/0.083) \times \ln(Mg/Ca/0.84)$, based on surface sediment samples from the tropical Atlantic and Caribbean and including the species *G. truncatulinoides* dextral and *G. crassaformis*. We chose this calibration over the species-specific *G. crassaformis* equation also in Regenberg et al. (2009) because it better represents the range of Mg/Ca values measured in our study, but this decision does not change our findings (Figure S1 in the supporting information). We assume a modern seawater Mg/Ca value (Mg/Ca_{sw}) for the late Pliocene/early Pleistocene ocean, and our reconstructed temperatures rest on the assumption that seawater Mg/Ca remained constant. This assumption is reasonable given the long residence times of Mg and Ca in the oceans (around 13 and 1 Ma, respectively) relative to the length of our study interval (~0.4 Ma). Lower Mg/Ca_{sw} reconstructed for the late Pliocene (~4.2 mol/mol vs 5.2 mol/mol today; Evans et al., 2016, and references therein) would have resulted in slightly warmer absolute temperatures calculated from our Mg/Ca data (+1.1 °C for *G. crassaformis* and +1 °C for *G. ruber*).

To calculate $\delta^{18}O$ residuals, that is, the local hydrographic component of planktic foraminiferal $\delta^{18}O$, we removed the measured temperature and global sea-level components from calcite $\delta^{18}O$. Seawater $\delta^{18}O$ ($\delta^{18}O_{sw}$) was first calculated from *G. ruber* and *G. crassaformis* $\delta^{18}O$ using the equation of Bemis et al. (1998). To extract the ice-volume component from $\delta^{18}O_{sw}$, we used the Mediterranean relative sea-level (RSL) record of Rohling et al. (2014) on its original Mediterranean chronology. The chronology applied to this RSL record (P. Wang et al., 2010) results in only minor discrepancies relative to the LR04 stack during our study interval (predominantly <3 kyr, increasing to 5 kyr during MIS 100 deglaciation). The RSL record was converted to permille units assuming a 0.008‰ increase in global seawater $\delta^{18}O$ per meter RSL fall (Schrag et al., 2002) and subtracted from our $\delta^{18}O_{sw}$ records to derive ice-volume corrected (IVC)-$\delta^{18}O_{sw}$.

2.5. Probabilistic Analysis of Uncertainties

Chronological and proxy-related uncertainties associated with the *T* and IVC-$\delta^{18}O_{sw}$ time series from Site U1313 were probabilistically evaluated using a Monte Carlo-style approach in MATLAB (Marino et al., 2015; Thirumalai et al., 2016). For the *T* reconstructions, input data for the Monte Carlo routine are the samples' ages with their uncertainties related to the LR04 chronology (Lisiecki & Raymo, 2005), the *G. ruber* and *G. crassaformis* Mg/Ca values with their analytical errors, and the Mg/Ca-T calibrations with their uncertainties (Anand et al., 2003; Regenberg et al., 2009). For the IVC-$\delta^{18}O_{sw}$ time series, input data are the ages and their uncertainties (as for SST) and the IVC-$\delta^{18}O_{sw}$ data and their propagated uncertainties (i.e., those associated with *T*, $\delta^{18}O$, and ice-volume reconstructions). For each of these *T* and IVC-$\delta^{18}O_{sw}$ time series, each data point is then separately and randomly sampled 10,000 times within their chronological and proxy uncertainties. Each of the 10,000 iterations is linearly interpolated and the probability distribution assessed at each time step, thereby determining the 68% (16–84th percentile) and 95% (2.5–97.5th percentile) probability intervals of the data. Finally, the probability maximum (PMAX; modal value) and its uncertainties (the 95% probability interval) are determined at each time step.

3. Results

3.1. Mg/Ca and Temperature

Globigerinoides ruber Mg/Ca varies between 3.75 and 4.25 mmol/mol during interglacials and 2.5 and 3 mmol/mol during glacials (Figure 3a). Minima (~2.5 mmol/mol) occur during cold stages associated with the largest-amplitude cycles in benthic $\delta^{18}O$ during our study interval, MIS G6, 104, 100, 98, and 96 (compare Figures 3a and 3c). *Globorotalia crassaformis* Mg/Ca ratios are typically ~0.5 to 1 mmol/mol lower than those measured in contemporary *G. ruber* samples. Both species exhibit a similar amplitude of glacial-interglacial (G-IG) change (~1 to 1.25 mmol/mol; Figure 3a). Yet the *G. crassaformis* Mg/Ca record shows a markedly different evolution over our study interval compared to *G. ruber*, exhibiting a step shift toward lower glacial and interglacial Mg/Ca ratios from MIS 101 onward that is not apparent in the *G. ruber* record (Figure 3a). Mg/Ca ratios in *G. crassaformis* for interglacials are ~3 mmol/mol between MIS G11 and MIS 103 and ~2.5 mmol/mol between

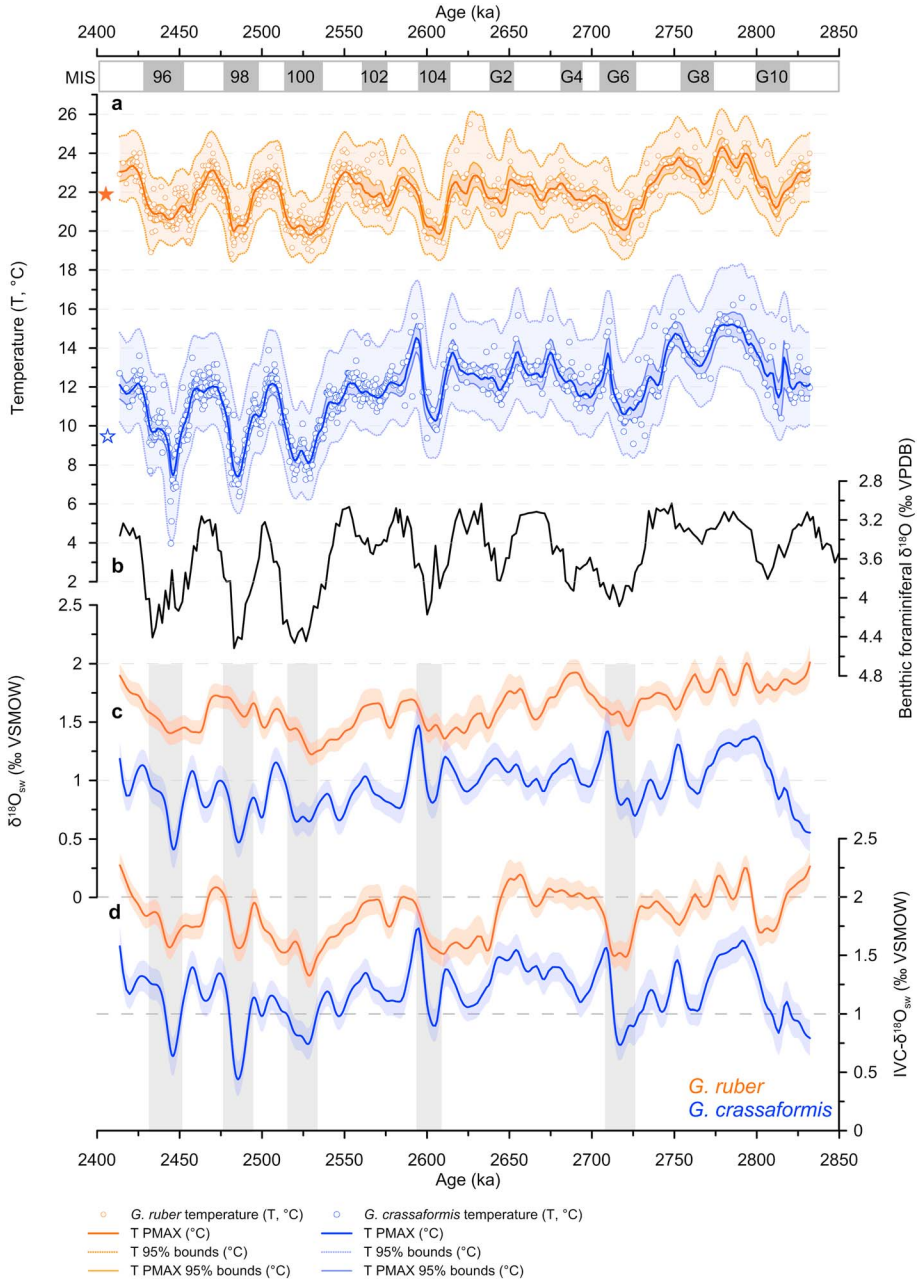

Figure 4. (a) Probabilistic temperature estimates based on Monte Carlo analysis of Mg/Ca data for *G. ruber* (orange) and *G. crassaformis* (blue) at Site U1313 (see legend). Orange star shows modern summer (Jun-Sept) sea surface temperature, and blue star shows modern mean annual temperature at 700-m depth above Site U1313, after Locarnini et al. (2013). (b) Benthic foraminiferal $\delta^{18}O$ record from Site U1313 (Bolton et al., 2010). (c) $\delta^{18}O_{sw}$ and (d) ice-volume corrected (IVC)-$\delta^{18}O_{sw}$ records for *G. ruber* and *G. crassaformis*. In (c) and (d), probability maximum (PMAX) curves from Monte Carlo analysis of the data are shown with their 95% probability interval. Gray bars denote larger-amplitude glacials where significant changes in IVC-$\delta^{18}O_{sw}$ occur (marine isotope stages G6, 104, 100, 98, and 96). VPDB = Vienna Pee Dee Belemnite, VSMOW = Vienna Standard Mean Ocean Water.

MIS 101 and MIS 95. Lowest Mg/Ca ratios in *G. crassaformis* (~1.5 mmol/mol) occur during glacials MIS 100, 98, and 96, whereas the preceding large-amplitude glacials, MIS G6 and 104, have higher ratios (~2 mmol/mol).

Temperature estimates derived from Mg/Ca data (see methods) are plotted with their confidence limits in Figure 4a. PMAX *G. ruber* temperatures vary between 24 (MIS G9) and 20 °C (MIS G6, 104, 100, and 98). G-IG temperature change is generally 2–3 °C, with no clear secular change in G-IG amplitude. These

temperatures vary around the modern summer (JJA) SST value of 22 °C near Site U1313 (Locarnini et al., 2013), consistent with peak August abundances of *G. ruber* in the region (Schiebel & Hemleben, 2000). The warmest SSTs recorded by *G. ruber* in our record (during interglacial MIS G9) are ~2 °C higher than today and fall in the range of midlatitude North Atlantic summer SST anomalies reconstructed for the Pliocene (Dowsett et al., 2011).

PMAX temperatures from *G. crassaformis* vary between 15°C (MIS G9) and 8 °C (MIS 100, 98, and 96; Figure 4a). G-IG temperature change reaches 4 °C during the larger-amplitude glacials MIS G6, 104, 100, 98, and 96. Prior to MIS 100, *G. crassaformis* records significantly warmer glacials (>10 °C) than thereafter (~8 °C), highlighting a prominent cooling that separate glacials before and after 2.55 Ma. Similarly, IG temperatures are consistently warmer before MIS 101 (>14 °C) than thereafter (~12 °C). These features occur regardless of which equation is used to convert *G. crassaformis* Mg/Ca to temperature (Figure S1).

3.2. Oxygen Isotopes and Residuals

Overall, the pattern of change in $\delta^{18}O$ for both planktic species is similar to that seen in the two Mg/Ca time series (Figure 3). *G. ruber* $\delta^{18}O$ varies between −0.25‰ and 1‰, with interglacial values of around −0.25‰ and glacial values of ~0.5‰ (highest values of 0.75–1‰ occur during MIS 98). *Globorotalia crassaformis* $\delta^{18}O$ show greater variability ranging from 1‰ to 2.5‰ and values that are higher (by ~1.25‰ to 1.5‰) than *G. ruber* $\delta^{18}O$. The prominent cooling in glacial temperatures as registered by *G. crassaformis* at 2.55 Ma (MIS 101; Figure 3b) is paralleled by an increase in glacial *G. crassaformis* $\delta^{18}O$. Between MIS 101 and 95, G-IG amplitude in $\delta^{18}O$ is ~0.25‰ greater for *G. crassaformis* than for *G. ruber* (Figure 3b). Subsurface $\delta^{18}O_{sw}$ as determined using *G. crassaformis* varies in the range 0.5‰ to 1.5‰, with minima in MIS G6, 104, 100, 98, and 96 (~0.6‰ excursions; Figure 4c). Surface (*G. ruber*) $\delta^{18}O_{sw}$ varies between 1.25‰ and 2‰, and lower-amplitude negative excursions (<0.4‰) are recorded during MIS G6, 104, 100, and 96 relative to in *G. crassaformis* $\delta^{18}O_{sw}$. IVC-$\delta^{18}O_{sw}$ records for both species are shown in Figure 4d. Removal of the ice-volume component from the $\delta^{18}O_{sw}$ records amplifies the decreases recorded during larger glacials, most notably MIS 100, 96, and 98 during which the largest sea level falls in our study interval occur.

3.3. *Neogloboquadrina atlantica* Abundances

Neogloboquadrina atlantica is present in very low numbers during glacials MIS G6, G4, and G2 (<1% of total planktic foraminifera, <50 *N. atlantica*/g) and in low numbers during glacials MIS 104, 100, 98, and 96 (<4% and <200 *N. atlantica*/g; Figure 5). *Neogloboquadrina atlantica* is otherwise absent during the study interval. Only the left-coiling morphotype was found in the samples studied. Percent and numbers per gram records display similar trends, with peak abundances of ~4% or ~200 *N. atlantica*/g during MIS 100 and MIS 104. These abundances are much lower than those in coeval sediments from sites further north (48–56°N) containing 20–70% *N. atlantica* (Dowsett et al., 2015; Loubere, 1988; Loubere & Moss, 1986; Raymo et al., 1986). The earliest appearance of *N. atlantica* during MIS G6 coincides with the first trace occurrences of IRD in Site U1313 sediments (Bolton et al., 2010; Lang et al., 2016). However, the relative amplitude of glacial peaks is not always consistent between the two proxy records, most notably during MIS 104 when *N. atlantica* abundances reach ~200 individuals per gram and IRD abundances are near zero (Figures 5d and 5e).

4. Discussion

4.1. Surface Hydrographic Changes

Our new high-resolution *G. ruber* Mg/Ca summer SST record (Figures 4 and 5) confirms a previous observation (Friedrich et al., 2013) that IG-G cycles in summer SSTs were modest during iNHG at Site U1313 (2–3 °C), and it also shows that glacial SSTs were >6 °C warmer than during the LGM. Friedrich et al. (2013) argue that this demonstrates that the NAC and Subarctic Front remained north of ~41°N throughout iNHG. Conversely, higher-amplitude cooling (5–6 °C) during some cold stages estimated from proxies that track mean annual (e.g., alkenones; Naafs et al., 2010) or spring (e.g., *Globigerina bulloides* Mg/Ca) SST at Site U1313 has been interpreted to suggest that the Subarctic Front was close to our study site during glacials from MIS G6 (Naafs et al., 2010) or MIS 104 (Hennissen et al., 2014) onward (Figure 5c). The greater magnitude of glacial cooling estimated from proxies tracking mean annual or spring SST at Site U1313 was interpreted to reflect increased seasonality, driven by intense winter cooling, that developed alongside large Northern Hemisphere ice sheets during iNHG (Friedrich et al., 2013; Hennissen et al., 2015). However, a situation where the Subarctic

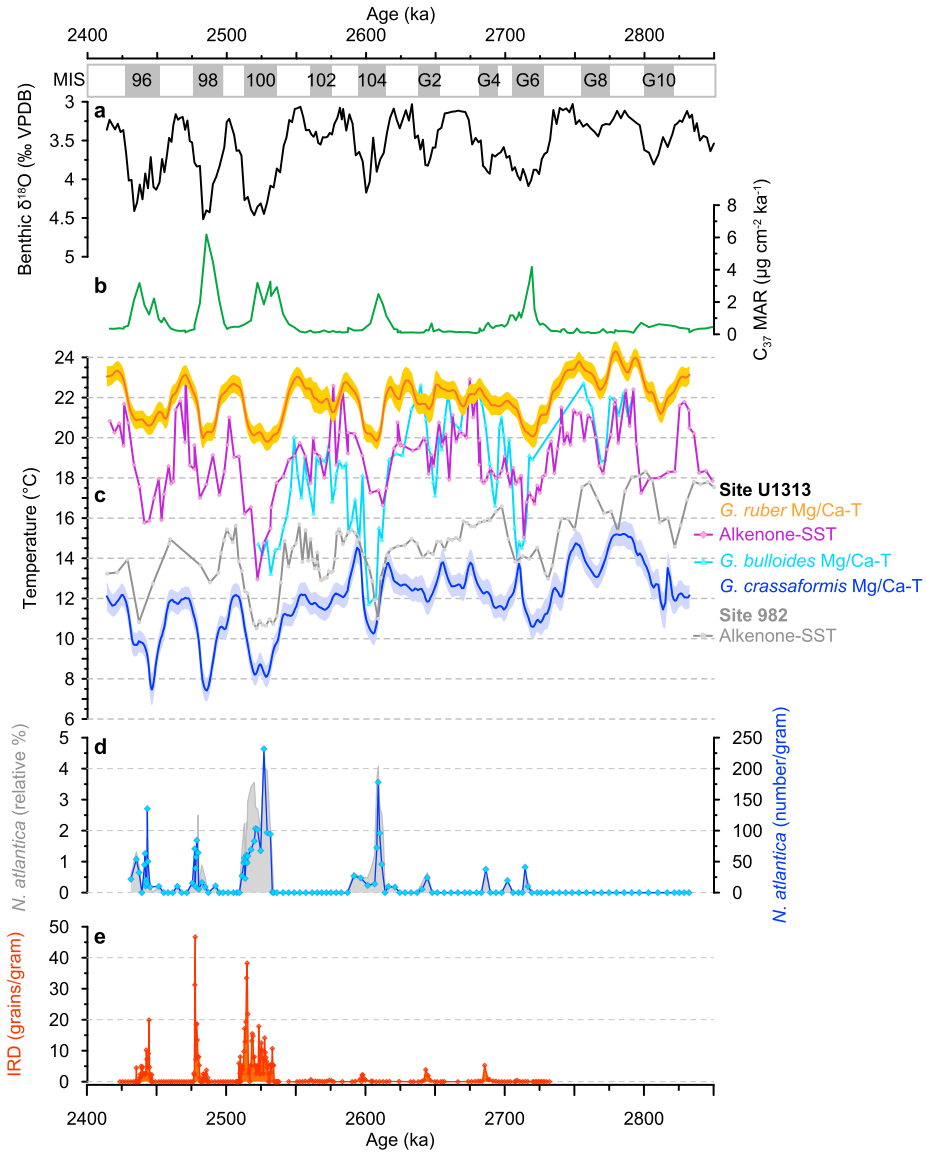

Figure 5. Temperature, productivity, *N. atlantica* abundance, and ice-rafted detritus (IRD) records from Site U1313: (a) benthic foraminiferal $\delta^{18}O$ (Bolton et al., 2010), (b) C_{37} alkenone mass accumulation rate (MAR) record of export productivity (Naafs et al., 2010), (c) Temperature records for *G. ruber* and *G. crassaformis* (only probability maximum and its 95% confidence limits are shown; this study), alkenone-based sea-surface temperature (SST; Naafs et al., 2010), and *Globigerina bulloides* Mg/Ca temperature (Hennissen et al., 2014). Because the *G. bulloides* data were generated on samples from Hole U1313C only, including samples from core sections that are outside of the Site U1313 primary splice, we retuned the benthic foraminiferal $\delta^{18}O$ record from Hole U1313C (Hennissen et al., 2014) to the benthic $\delta^{18}O$ record based on samples from the primary splice (Bolton et al., 2010) so that records are on the same age model (see supporting information Figure S3). Also shown are alkenone-based SSTs from ODP Site 982 (Lawrence et al., 2009). (d) *Neogloboquadrina atlantica* relative abundance (gray) and numbers/gram sediment (blue) at Site U1313. (e) IRD abundance at Site U1313 (Bolton et al., 2010; Lang et al., 2016). VPDB = Vienna Pee Dee Belemnite.

Front reached the midlatitudes during winter but not during summer has no analogy in the LGM. SST reconstructions for the LGM from ~40°N show no amplification of cooling in winter relative to summer (Chapman et al., 2000), and LGM reconstructions of latitudinal SST gradients show that the Subarctic Front, represented by closely spaced isotherms of 8–20 °C (summer) or 4–16 °C (winter), had the same latitudinal position in both seasons (37–45°N; Pflaumann et al., 2003; Waelbroeck et al., 2009). These important observations imply that, under LGM-like conditions, large SST decreases associated with southward migrations of the Subarctic Front should be detectable in both summer and winter SSTs. Given that the

coldest glacial summer *G. ruber*-based SSTs during our study interval (~19 °C) were >6 °C warmer than LGM summer SSTs at the same latitude (Chapman et al., 2000; Pflaumann et al., 2003), the available SST data strongly suggest that surface gyre circulation patterns in the midlatitude North Atlantic were not LGM-like during iNHG cold stages.

Our suggestion that Subarctic Front position in the glacial North Atlantic during iNHG was not analogous to the LGM is supported by our new record of *N. atlantica*(s) abundance in Site U1313 sediments. Similar to *N. pachyderma*(s) in the late Pleistocene, *N. atlantica* has been suggested to be a useful indicator of the presence of subpolar waters in the Pliocene North Atlantic (Becker et al., 2006). The association of *N. atlantica* with subpolar waters during the Pliocene is supported by its midlatitude to high-latitude distribution in spatial maps of its abundance in North Atlantic sediments deposited during the mid-Piacenzian warm period (Dowsett & Robinson, 2007; Robinson, 2018; Figure 2c). Furthermore, its presence in sediments deposited in the central and eastern Mediterranean during MIS G6, 100, 98, and 96 has been cited as evidence that the Subarctic Front first extended to the midlatitudes during cold stages from ~2.7 Ma (Becker et al., 2005; Lourens et al., 1992, 1996; Zachariasse et al., 1990). In contrast, the trace numbers of *N. atlantica* tests in sediments deposited at Site U1313 during MIS G6, G4, and G2 (Figure 5d) highlight that Subarctic Front waters did not lie above our study site during these glacials, a finding consistent with the conclusions of Hennissen et al. (2014). Significant numbers of *N. atlantica* do occur in Site U1313 sediments during glacials MIS 104, 100, 98, and 96, yet its abundance is generally low (<2%, with maxima of ~4% during MIS 104 and 100; Figure 5d) compared to abundances of *N. pachyderma*(s) observed in sediments deposited at 40–41°N during ambient (non-Heinrich event) glacial conditions of the LGM (~10%; Chapman et al., 2000; Smith et al., 2013; Figure 2b). The low abundances of *N. atlantica* at ~41°N imply that, while some subpolar surface water did mix into the mainly subtropical water mass above Site U1313 during cold stages from ~2.6 Ma, especially during MIS 104 and 100, subpolar water masses did not reach as far south during iNHG as during the LGM. In this interpretation, Site U1313 remained at the southern boundary of the mixing zone between subpolar and subtropical waters during major iNHG glacials (during both summer and winter) rather than in a truly subpolar surface water mass. This suggestion is supported by our observation that surface water IVC-$\delta^{18}O_{sw}$ decreases modestly (by at most 0.5‰) during glacials at Site U1313 (Figure 4d), compared to the amplitude of change observed in this region between the LGM (under ambient glacial conditions) and the Holocene (~0.75‰) in nearby Site SU90-08 (supporting information Figure S2; Cortijo et al., 1997; Vidal et al., 1997; Villanueva, Grimalt, Labeyrie, et al., 1998). One mechanism by which subpolar waters could have reached the latitude of Site U1313 during prominent glacials from MIS 104, despite the Subarctic Front being further north, is via cold-core rings (eddies), which form in meanders of the Gulf Stream and NAC, eventually detaching and transporting large parcels of subpolar water through the adjacent subtropical water mass (Mittelstaedt, 1987; The Ring Group, 1981).

Relative abundances of *N. atlantica* reach 15% to 30% in central and eastern Mediterranean sediments deposited during MIS G6, 100, 98, and 96 (Becker et al., 2005; Lourens et al., 1992, 1996; Zachariasse et al., 1990). These high abundances relative to our Site U1313 record cannot be explained by sedimentation rate differences (which are higher in the Mediterranean at this time). The presence of *N. atlantica* at Site U1313 during MIS 104, when it was absent in the Mediterranean, could be explained if subpolar waters extended to 41°N during this cold stage, but not into the Mediterranean. The presence of *N. atlantica* in the Mediterranean during MIS G6 while it is almost absent from Site U1313 sediments cannot, however, be explained by a plausible southward migration of the Subarctic Front. Although western Mediterranean climate was highly sensitive to North Atlantic cooling events and shifts in the Subarctic Front during the last glacial (Cacho et al., 2001; Rohling et al., 1998), it is unlikely that incursions of subpolar water reached the central and eastern Mediterranean, except potentially during the strongest Heinrich events (e.g., Cornuault et al., 2016; Grant et al., 2016). Rather than representing invasions resulting from direct subpolar water inflow (Becker et al., 2006; Spaak, 1982; Zachariasse et al., 1990), *N. atlantica* peaks in the Mediterranean during iNHG therefore likely reflect the development of specific temperature and nutrient conditions that favored the proliferation of indigenous but previously rare populations, as proposed for *N. pachyderma*(s) in the late Pleistocene western Mediterranean (Rohling et al., 1998).

During the LGM, IRD concentrations in sediments deposited at Site U1313 outside Heinrich events are ~40–50 grains/gram (Lang et al., 2016). Similar concentrations are first found in Site U1313 sediments during MIS 100 (Bolton et al., 2010). Iceberg calving models for the LGM suggest that the source of IRD to this region of

the North Atlantic is the Gulf of St. Lawrence in midlatitude North America (Bigg & Wadley, 2001). The absence of IRD at LGM-like concentrations during MIS 104, when *N. atlantica* abundances are as high as those during MIS 100, therefore does not necessarily imply that subpolar waters were absent at Site U1313 at this time, but rather that the source of IRD to this region of the subpolar Atlantic was absent until MIS 100, which is consistent with other evidence for the timing of the onset of midlatitude glaciation of North America (Balco & Rovey, 2010).

Finally, we briefly discuss the differences that exist in the amplitude of glacial cooling recorded by available SST proxies at Site U1313 during iNHG (Figure 5c). The abundance of *N. atlantica* in Site U1313 sediments increases significantly for the first time during MIS 104 (up to 4%), suggesting a small but detectable influence of subpolar surface waters at Site U1313 during this glacial. This finding is consistent with dinoflagellate evidence reported by Hennissen et al. (2014) that the first significant southward shift of the NAC occurred at this time. Summer SSTs based on *G. ruber* do not, however, show greater cooling during MIS 104 (~3 °C) compared to MIS G6 (3–4 °C). The same is true of alkenone SSTs, interpreted to reflect mean annual temperatures with a possible bias toward spring (Naafs et al., 2010), which show a ~4 °C cooling during both MIS G6 and 104. In contrast, *G. bulloides*-derived SSTs, interpreted to reflect spring temperatures (Hennissen et al., 2014), record a cooling of ~6 °C during MIS G6 and ~10 °C during MIS 104. These differences in SST cannot easily be reconciled by considering the different seasonal biases of the three proxies. Our *G. ruber* record is much higher resolution than the other two SST records, so the differences described above cannot be a product of sample aliasing. *G. bulloides* SSTs of 12 °C during MIS 104 are similar to *G. crassaformis*-derived temperatures at Site U1313 (thought to reflect 500–800-m water depth) and alkenone-derived SSTs at Site 982, located at 57°N (Figure 5c). If surface waters above Site U1313 were bathed in a pure subpolar water mass during MIS 104, as could be inferred from the relatively cold *G. bulloides* SST values for this glacial, then we would expect a far greater dominance of *N. atlantica* in Site U1313 sediments deposited at this time (e.g., $>$20% as seen north of 45–50°N during the warm Pliocene; Figure 2c). In light of these observations, we suggest that *G. bulloides* does not record a pure surface temperature signal at Site U1313 on orbital timescales over iNHG. *G. bulloides*, which is a nonsymbiont-bearing species, could have carried out significant vertical migrations in response to food supply and water column structure (Mortyn & Charles, 2003) and/or occupied a large depth range in the upper water column in spring, when deep mixing and storms simultaneously stimulate productivity and distribute planktic foraminifera down to depths of ~200 m (Schiebel et al., 1995, 1997). During MIS 104, when the subtropical gyre was displaced southward, this greater vertical distribution would have had a larger effect on reconstructed *G. bulloides* SSTs. Conversely, *G. ruber* was probably more restricted to the upper photic zone both by the late summer seasonal thermocline and by its photosynthetic symbionts.

4.2. Subsurface Hydrographic Changes

Southward migrations of the Subarctic Front on IG-G timescales could result in changes in the contribution of different water masses to the permanent pycnocline at 41°N (centered on 700–750 m; Feucher et al., 2016; Figure 1c). Hence, while the surface Subarctic Front may not have shifted as far south as Site U1313, as it appears to have done during the LGM, contractions of the subtropical gyre associated with southward migration of the NAC and Subarctic Front during iNHG glacials may have still occurred. These southward shifts could be recorded in our *G. crassaformis* data sets, because the depth profile of the subtropical gyre boundary is such that the mixing zone between subtropical and subpolar waters occurs further south at 500–800 m compared to at the surface (Figure 1c).

The permanent pycnocline is, by definition, a transitional zone with a significant vertical density gradient, so its temperature, salinity, and density primarily reflect mixing between water masses with more homogenous properties above and below it and the properties of these water masses. In the subtropical North Atlantic, mode waters above the pycnocline are made up of a variable mixture of subtropical mode water, North Atlantic central water, and subpolar mode water (SPMW), whereas waters below (~500–2,000 m) contain a mixture of Subarctic intermediate water, Labrador Sea water, Mediterranean outflow water, and Antarctic intermediate water (Talley et al., 2011; van Aken, 2000, 2001). Subtropical mode waters form in the western Atlantic between 35°N and 40°N, where isopycnals crop out at the surface and a combination of downward Ekman pumping and buoyancy flux drives water into the ocean interior along isopycnal surfaces (Keffer, 1985; Luyten et al., 1983; Sarmiento, 1983; Trossman et al., 2012). In the northeast Atlantic (~50–65°N),

SPMWs form during deep winter convection, primarily south of Iceland, and dominate the layer between the surface ocean and the permanent pycnocline in the subpolar gyre (Brambilla et al., 2008; Brambilla & Talley, 2008; McCartney & Talley, 1982; Trossman et al., 2012). *Globorotalia crassaformis* is thought to calcify in the permanent pycnocline layer of the subtropical gyre. During our study interval, Mg/Ca temperatures for this species are between 8 and 15 °C, with IG-G oscillations of up to 4 °C superimposed on a longer-term cooling trend (Figure 4a).

Several lines of evidence point to a dominant influence of SPMWs in the permanent pycnocline at Site U1313 throughout iNHG and especially during pronounced glacials. First, the long-term cooling trend recorded by *G. crassaformis* at our study site is strikingly similar to the trend in an alkenone-based SST record from ODP Site 982 (57°N; Lawrence et al., 2009)—in the formation region of SPMWs (Figure 5c). The temperature difference of ~2 °C between the surface at Site 982 and the pycnocline at Site U1313 is close to the modern difference (Locarnini et al., 2013), and oceanographic data from the midlatitude eastern North Atlantic support a subpolar source for waters in the permanent pycnocline today (van Aken, 2001). Second, subpolar waters have a lighter $\delta^{18}O_{sw}$ signature than subtropical waters (LeGrande & Schmidt, 2006), and a strong imprint of SPMWs on *G. crassaformis* test geochemistry at Site U1313 can therefore be inferred from $\delta^{18}O_{sw}$ values for this species because they are lighter than those calculated for *G. ruber* throughout the record (Figures 4c and 4d). Lastly, because of the sensitivity of *G. crassaformis* depth habitat to small north-south movements of the subtropical gyre boundary (Figure 1c), we propose that the larger amplitude temperature and $\delta^{18}O_{sw}$ decreases recorded by this species relative to *G. ruber* during prominent glacials from MIS 104 onward (Figure 4) reflect equatorward shifts of the subtropical gyre boundary that led to increased SPMW influence on the permanent pycnocline above Site U1313.

In summary, while we infer that surface waters above Site U1313 were further south in the mixing zone between subtropical and subpolar waters during glacials throughout iNHG than during the LGM, we suggest that contractions of the subtropical gyre during prominent glacials from MIS 104 onward (when *G. crassaformis*-based temperatures show greater cooling than *G. ruber*-based SSTs) were recorded in the permanent pycnocline against a backdrop of long-term regional high-latitude North Atlantic sea-surface cooling (Herbert et al., 2016; Lawrence et al., 2009) that was transferred to the midlatitude North Atlantic via SPMWs. We also note that the global deep-sea benthic $\delta^{18}O$ deconvolution of Rohling et al. (2014) indicates a mean ~2 °C deep-sea cooling through our study interval, which suggests similar polar cooling in both hemispheres.

4.3. Implications

The first sudden increase in abundance of *N. atlantica* in sediments deposited at Site U1313 during MIS 104, at ~2.6 Ma, is consistent with the timing inferred for the first southward deflection of the NAC and Subarctic Front based on dinoflagellate cyst assemblage data (Hennissen et al., 2014). Naafs et al. (2010) used the onset of large export productivity peaks and large SST decreases during glacials from ~2.7 Ma at Site U1313 (Figure 5b) to suggest that nutrient-rich surface waters associated with the Subarctic Front first influenced waters above Site U1313 during cold stages from MIS G6 onward. The near-absence of *N. atlantica* in sediments deposited at Site U1313 during MIS G6, despite enhanced primary productivity, implies, however, that nutrient-rich subpolar waters were largely absent at ~41°N at this time and that *N. atlantica* abundance in the midlatitude North Atlantic was not related to nutrient availability. It also suggests that the onset of high primary productivity during glacials from MIS G6 onward at Site U1313 was driven by factor(s) additional to direct mixing of subpolar surface water with subtropical water masses.

A more compressed North Atlantic subtropical gyre and an equatorward shift of westerly wind belts and the northern gyre boundary due to surface cooling have been hypothesized for the LGM (Billups & Schrag, 2000; Keffer et al., 1988; Slowey & Curry, 1995) and for glacials after 2.7 Ma (MIS G6) during iNHG (Lawrence et al., 2013). Our *G. crassaformis* records support the hypothesis that contractions of the subtropical gyre occurred during prominent iNHG glacials. Thus, shoaling of the subtropical gyre thermocline and nutricline may have increased the advection of nutrient-rich waters to the photic zone, stimulating primary productivity at Site U1313 from MIS G6 onward (Lawrence et al., 2013). Subantarctic Mode Waters and Antarctic intermediate waters feed nutrients into the North Atlantic subtropical thermocline via intermediate water circulation pathways (Sarmiento et al., 2004) and have been implicated in productivity increases during iNHG at Site U1313 (Lawrence et al., 2013). However, the strong imprint of SPMWs on our permanent pycnocline records implies that southern-sourced intermediate waters played only a minor role in driving productivity at the northern

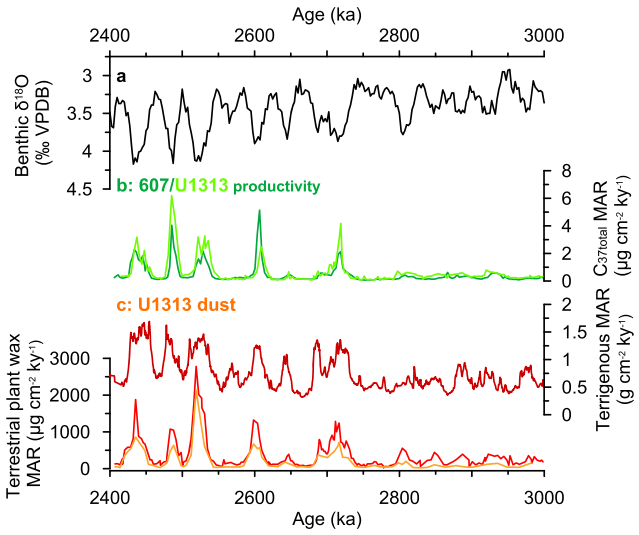

Figure 6. Export productivity and dust proxy records from Sites U1313 (607) between 3 and 2.4 Ma. (a) Benthic foraminiferal $\delta^{18}O$ global stack (Lisiecki & Raymo, 2005), (b) C_{37} alkenone mass accumulation rates (MAR) at Deep Sea Drilling Project Site 607 (dark green; Lawrence et al., 2013) and Integrated Ocean Drilling Program Site U1313 (light green; Naafs et al., 2010), and (c) aeolian dust proxies at Site U1313: terrigenous MAR (dark red; Lang et al., 2014) and terrestrial plant wax MAR: *n*-alkanes (red) and *n*-alkan-1-ols (orange; Naafs et al., 2012). VPDB = Vienna Pee Dee Belemnite.

gyre boundary. Perhaps more importantly, proxy records for dust deposition at Site U1313 show a large increase during glacials from MIS G6 onward (Lang et al., 2014; Naafs et al., 2012) (Figure 6). Today, phytoplankton growth in the region of Site U1313 is limited by iron (Moore et al., 2006), which is primarily supplied to the central North Atlantic by aeolian pathways. Therefore, an increase in dustiness during glacials from MIS G6 onward due to the aridification of North America may have alleviated iron limitation on phytoplankton growth and in part driven the trends in export productivity observed. A second, potentially significant, source of nutrients to surface waters above Site U1313 during prominent iNHG glacials, when the Subarctic Front was closest to 41°N, could have been cold-core eddies. Mesoscale eddies, measuring tens to hundreds of kilometers in diameter and evident down to depths of several thousand meters, break off from the Subarctic Front and meander into subtropical waters, resulting in episodic nutrient injection and increased new primary productivity in the midlatitude North Atlantic (Falkowski et al., 1991; Lochte & Pfannkuche, 1987; Mittelstaedt, 1987; Oschlies & Garçon, 1998).

The geometry of North American ice sheets forced a zonal wind pattern that is responsible for the position of the Subpolar Front during glaciations and for bringing polar air into contact with larger areas of the North Atlantic Ocean (Clark et al., 1999; Imbrie et al., 1993; Keffer et al., 1988). Our observation that subpolar surface waters did not influence Site U1313 strongly until MIS 104, ~2.6 Ma, implies that continental ice sheets on North America were not large enough to significantly modify North Atlantic surface circulation until this time. It has been proposed that Northern Hemisphere continental ice-sheets were less tall (or lower-slung) during iNHG relative to the LGM (Bailey et al., 2010). If a low-slung North American ice-sheet complex grew during iNHG cold stages, it might help explain why subpolar waters apparently penetrated less far south during these glaciations relative to the LGM, since the lower height of the ice sheets would have modified atmospheric circulation, and therefore surface ocean gyre circulation, to a lesser degree.

5. Conclusions

We present new records of surface and subsurface water properties based on planktic foraminiferal geochemistry and abundance from IODP Site U1313 that shed light on the evolution of midlatitude North Atlantic paleoceanography and the position of the Subarctic Front during the iNHG. At our study site (Lat. 41°N, Long. 32.5°W), glacial surface ocean cooling of ~3 °C (*G. ruber* Mg/Ca) or 4–6 °C (alkenones; Naafs et al., 2010) is modest compared to the 8–9 °C warming observed between the LGM and the Holocene (alkenones; Naafs et al., 2012). Abundances of the planktic foraminifera *N. atlantica* in U1313 sediments deposited during the late Pliocene and early Pleistocene reflect a small but significant increase in the influence of surface subpolar waters in the midlatitude North Atlantic during prominent glacials from MIS 104 onward. In the subsurface, these changes are associated with ~4 °C cooling and ice-volume corrected-$\delta^{18}O_{sw}$ decreases of $>$0.5‰, in the permanent pycnocline (as recorded by *G. crassaformis*), which are interpreted to reflect contractions of the subtropical gyre during prominent glacials from this time. The secular cooling recorded by *G. crassaformis* reflects regional northern high latitude trends at this time (Herbert et al., 2016; Lawrence et al., 2009), suggesting a strong imprint of subpolar mode waters. Based on these findings, we infer that the Subarctic Front did not adopt a LGM-like position during iNHG glacials and that surface waters above Site U1313 remained on the southern fringe of the mixing zone between subtropical and subpolar waters throughout our study interval. The fact that the first significant influence of nutrient-rich subpolar surface waters at Site U1313 (during MIS 104) post-dates the onset of major glacial productivity peaks at our site (during MIS G6) by ~120 kyr implies that changes in surface gyre circulation at this time were not the sole driver of primary productivity in the midlatitude North Atlantic during iNHG. We propose that additional factors, namely, a significant increase in dust delivery from North America to the midlatitude North Atlantic during

glacials from MIS G6 onward and the influence of cold-core eddies originating from a more proximal NAC, helped promote an increase in export productivity at this time.

Acknowledgments
This research uses samples provided by the IODP, which is sponsored by the U.S. National Science Foundation and participating countries under management of Joint Oceanographic Institutions, Inc. We thank the shipboard party of IODP Expedition 306 and A. Wuelbers and W. Hale for their help at the Bremen Core Repository. We thank David Naafs and an anonymous reviewer for comments that helped to improve this manuscript. Funding for this research was provided by IODP France (C. T. B.) and the German Research Foundation (DFG) (grant OF 2544/2 to O. F.). I. B. is grateful to the UK IODP for financial support for shipboard and post-cruise participation in IODP Exp. 306. C. T. B., K. T., T. D. G., L. V., C. S., and M. E. acknowledge OSU Pythéas. M. M. R. acknowledges support by the USGS Land Change Science Program. Any use of trade, firm, or product names is for descriptive purposes only and does not imply endorsement by the U.S. Government. P. A. W. acknowledges NERC UK IODP NE/F00141X/1 and a Royal Society Wolfson Merit Award. All new data presented here are available at https://doi.pangaea.de/10.1594/PANGAEA.892805.

References

van Aken, H. M. (2000). The hydrography of the mid-latitude Northeast Atlantic Ocean II: The intermediate water masses. *Deep Sea Research Part I: Oceanographic Research Papers*, *47*(5), 789–824. https://doi.org/10.1016/S0967-0637(99)00112-0

van Aken, H. M. (2001). The hydrography of the mid-latitude northeast Atlantic Ocean—Part III: The subducted thermocline water mass. *Deep Sea Research Part I: Oceanographic Research Papers*, *48*(1), 237–267. https://doi.org/10.1016/S0967-0637(00)00059-5

Anand, P., Elderfield, H., & Conte, M. H. (2003). Calibration of Mg/Ca thermometry in planktonic foraminifera from a sediment trap time series. *Paleoceanography*, *18*(2), 1050. https://doi.org/10.1029/2002PA000846

Arnold, T. E., Diefendorf, A. F., Brenner, M., Freeman, K. H., & Baczynski, A. A. (2018). Climate response of the Florida Peninsula to Heinrich events in the North Atlantic. *Quaternary Science Reviews*, *194*, 1–11. https://doi.org/10.1016/j.quascirev.2018.06.012

Aurahs, R., Treis, Y., Darling, K., & Kucera, M. (2011). A revised taxonomic and phylogenetic concept for the planktonic foraminifer species *Globigerinoides ruber* based on molecular and morphometric evidence. *Marine Micropaleontology*, *79*(1-2), 1–14. https://doi.org/10.1016/j.marmicro.2010.12.001

Bailey, I., Bolton, C. T., DeConto, R. M., Pollard, D., Schiebel, R., & Wilson, P. A. (2010). A low threshold for North Atlantic ice rafting from "low-slung slippery" late Pliocene ice sheets. *Paleoceanography*, *25*, PA1212. https://doi.org/10.1029/2009PA001736

Balco, G., & Rovey, C. W. (2010). Absolute chronology for major Pleistocene advances of the Laurentide Ice Sheet. *Geology*, *38*(9), 795–798. https://doi.org/10.1130/G30946.1

Bard, E., Arnold, M., Maurice, P., Duprat, J., Moyes, J., & Duplessy, J.-C. (1987). Retreat velocity of the North Atlantic polar front during the last deglaciation determined by ^{14}C accelerator mass spectrometry. *Nature*, *328*(6133), 791–794. https://doi.org/10.1038/328791a0

Barker, S., Greaves, M., & Elderfield, H. (2003). A study of cleaning procedures used for foraminiferal Mg/Ca paleothermometry. *Geochemistry, Geophysics, Geosystems*, *4*(9), 8407. https://doi.org/10.1029/2003GC000559

Bé, A. W. H., & Hutson, W. H. (1977). Ecology of planktonic foraminifera and biogeographic patterns of life and fossil assemblages in the Indian Ocean. *Micropaleontology*, *23*(4), 369–414. https://doi.org/10.2307/1485406

Becker, J., Lourens, L. J., Hilgen, F. J., van der Laan, E., Kouwenhoven, T. J., & Reichart, G.-J. (2005). Late Pliocene climate variability on Milankovitch to millennial time scales: A high-resolution study of MIS100 from the Mediterranean. *Palaeogeography, Palaeoclimatology, Palaeoecology*, *228*(3–4), 338–360. https://doi.org/10.1016/j.palaeo.2005.06.020

Becker, J., Lourens, L. J., & Raymo, M. E. (2006). High-frequency climate linkages between the North Atlantic and the Mediterranean during marine oxygen isotope stage 100 (MIS100). *Paleoceanography*, *21*, PA3002. https://doi.org/10.1029/2005PA001168

Bemis, B. E., Spero, H. J., Bijma, J., & Lea, D. W. (1998). Reevaluation of the oxygen isotopic composition of planktonic foraminifera: Experimental results and revised paleotemperature equations. *Paleoceanography*, *13*, 150–160. https://doi.org/10.1029/98PA00070

Berggren, W. (1972). Cenozoic biostratigraphy and paleobiogeography of the North Atlantic. *Initial Reports of the Deep Sea Drilling Project*, *12*(14), 965–1001.

Bigg, G. R., & Wadley, M. R. (2001). The origin and flux of icebergs released into the Last Glacial Maximum Northern Hemisphere oceans: The impact of ice-sheet topography. *Journal of Quaternary Science*, *16*(6), 565–573. https://doi.org/10.1002/jqs.628

Bijma, J., Faber, W. W., & Hemleben, C. (1990). Temperature and salinity limits for growth and survival of some planktonic foraminifers in laboratory cultures. *Journal of Foraminiferal Research*, *20*(2), 95–116. https://doi.org/10.2113/gsjfr.20.2.95

Billups, K., & Schrag, D. (2000). Surface ocean density gradients during the Last Glacial Maximum. *Paleoceanography*, *15*, 110–123. https://doi.org/10.1029/1999PA000405

Bolton, C. T., Wilson, P. A., Bailey, I., Friedrich, O., Beer, C. J., Becker, J., et al. (2010). Millennial-scale climate variability in the subpolar North Atlantic Ocean during the late Pliocene. *Paleoceanography*, *25*, PA4218. https://doi.org/10.1029/2010PA001951

Brambilla, E., & Talley, L. D. (2008). Subpolar mode water in the northeastern Atlantic: 1. Averaged properties and mean circulation. *Journal of Geophysical Research*, *113*, C04025. https://doi.org/10.1029/2006JC004062

Brambilla, E., Talley, L. D., & Robbins, P. E. (2008). Subpolar mode water in the northeastern Atlantic: 2. Origin and transformation. *Journal of Geophysical Research*, *113*, C04026. https://doi.org/10.1029/2006JC004063

Cacho, I., Grimalt, J. O., Canals, M., Sbaffi, L., Shackleton, N. J., Schönfeld, J., & Zahn, R. (2001). Variability of the western Mediterranean Sea surface temperature during the last 25,000 years and its connection with the Northern Hemisphere climatic changes. *Paleoceanography*, *16*, 40–52. https://doi.org/10.1029/2000PA000502

Cacho, I., Grimalt, J. O., Pelejero, C., Canals, M., Sierro, F. J., Flores, J. A., & Shackleton, N. (1999). Dansgaard-Oeschger and Heinrich event imprints in Alboran Sea paleotemperatures. *Paleoceanography*, *14*, 698–705. https://doi.org/10.1029/1999PA900044

Calvo, E., Villanueva, J., Grimalt, J. O., Boelaert, A., & Labeyrie, L. (2001). New insights into the glacial latitudinal temperature gradients in the North Atlantic. Results from UK′ 37 sea surface temperatures and terrigenous inputs. *Earth and Planetary Science Letters*, *188*(3-4), 509–519. https://doi.org/10.1016/S0012-821x(01)00316-8

Chapman, M., & Maslin, M. A. (1999). Low-latitude forcing of meridional temperature and salinity gradients in the subpolar North Atlantic and the growth of glacial ice sheets. *Geology*, *27*(10), 875–878. https://doi.org/10.1130/0091-7613

Chapman, M., Shackleton, N. J., & Duplessy, J.-C. (2000). Sea surface temperature variability during the last glacial–interglacial cycle: Assessing the magnitude and pattern of climate change in the North Atlantic. *Palaeogeography, Palaeoclimatology, Palaeoecology*, *157*(1-2), 1–25. https://doi.org/10.1016/S0031-0182(99)00168-6

Clark, P. U., Alley, R. B., & Pollard, D. (1999). Northern Hemisphere ice-sheet influences on global climate change. *Science*, *286*(5442), 1104–1111. https://doi.org/10.1126/science.286.5442.1104

Cléroux, C., deMenocal, P., Arbuszewski, J., & Linsley, B. (2013). Reconstructing the upper water column thermal structure in the Atlantic Ocean. *Paleoceanography*, *28*, 503–516. https://doi.org/10.1002/palo.20050

CLIMAP (1981). *Seasonal reconstructions of the Earth's surface at the Last Glacial Maximum*. Boulder, Colorado: Geological Society of America.

Cornuault, M., Vidal, L., Tachikawa, K., Licari, L., Rouaud, G., Sonzogni, C., & Revel, M. (2016). Deep water circulation within the eastern Mediterranean Sea over the last 95 kyr: New insights from stable isotopes and benthic foraminiferal assemblages. *Palaeogeography, Palaeoclimatology, Palaeoecology*, *459*, 1–14. https://doi.org/10.1016/j.palaeo.2016.06.038

Cortijo, E., Labeyrie, L., Vidal, L., Vautravers, M., Chapman, M., Duplessy, J.-C., et al. (1997). Changes in sea surface hydrology associated with Heinrich event 4 in the North Atlantic Ocean between 40 and 60 N. *Earth and Planetary Science Letters*, *146*(1), 29–45.

Dickson, R. R., Meincke, J., Malmberg, S.-A., & Lee, A. J. (1988). The "great salinity anomaly" in the northern North Atlantic 1968–1982. *Progress in Oceanography*, *20*(2), 103–151. https://doi.org/10.1016/0079-6611(88)90049-3

Dowsett, H. J., Haywood, A. M., Valdes, P. J., Robinson, M. M., Lunt, D. J., Hill, D. J., et al. (2011). Sea surface temperatures of the mid-Piacenzian Warm Period: A comparison of PRISM3 and HadCM3. *Palaeogeography, Palaeoclimatology, Palaeoecology*, *309*(1-2), 83–91. https://doi.org/10.1016/j.palaeo.2011.03.016

Dowsett, H. J., & Poore, R. Z. (1990). A new planktic foraminifer transfer function for estimating Pliocene–Holocene paleoceanographic conditions in the North Atlantic. *Marine Micropaleontology*, *16*(1–2), 1–23. https://doi.org/10.1016/0377-8398(90)90026-I

Dowsett, H. J., & Robinson, M. M. (2007). Mid-Pliocene planktic foraminifer assemblage of the North Atlantic Ocean. *Micropaleontology*, *53*(1–2), 105–126. https://doi.org/10.2113/gsmicropal.53.1-2.105

Dowsett, H. J., Robinson, M. M., & Foley, K. (2015). A global planktic foraminifer census data set for the Pliocene ocean. *Scientific Data*, *2*, 150076. https://doi.org/10.1038/sdata.2015.76

Evans, D., Brierley, C., Raymo, M. E., Erez, J., & Müller, W. (2016). Planktic foraminifera shell chemistry response to seawater chemistry: Pliocene–Pleistocene seawater Mg/Ca, temperature and sea level change. *Earth and Planetary Science Letters*, *438*, 139–148. https://doi.org/10.1016/j.epsl.2016.01.013

Eynaud, F., De Abreu, L., Voelker, A., Schönfeld, J., Salgueiro, E., Turon, J. L., et al. (2009). Position of the Polar Front along the western Iberian margin during key cold episodes of the last 45 ka. *Geochemistry, Geophysics, Geosystems*, *10*, Q07U05. https://doi.org/10.1029/2009GC002398

Ezard, T. H., Edgar, K. M., & Hull, P. M. (2015). Environmental and biological controls on size-specific $\delta^{13}C$ and $\delta^{18}O$ in recent planktonic foraminifera. *Paleoceanography*, *30*, 151–173. https://doi.org/10.1002/2014PA002735

Falkowski, P. G., Ziemann, D., Kolber, Z., & Bienfang, P. K. (1991). Role of eddy pumping in enhancing primary production in the ocean. *Nature*, *352*(6330), 55–58. https://doi.org/10.1038/352055a0

Feucher, C., Maze, G., & Mercier, H. (2016). Mean structure of the North Atlantic subtropical permanent pycnocline from in-situ observations. *Journal of Atmospheric and Oceanic Technology*, *33*(6), 1285–1308. https://doi.org/10.1175/JTECH-D-15-0192.1

Foley, K. M., Dowsett, Harry, & Robinson, Marci. (2015). A global planktic foraminifer census dataset for the Pliocene ocean, National Climate Data Center. https://www.ncdc.noaa.gov/paleo/study/19281

Friedrich, O., Schiebel, R., Wilson, P. A., Weldeab, S., Beer, C. J., Cooper, M. J., & Fiebig, J. (2012). Influence of test size, water depth, and ecology on Mg/Ca, Sr/Ca, $\delta^{18}O$ and $\delta^{13}C$ in nine modern species of planktic foraminifers. *Earth and Planetary Science Letters*, *319-320*, 133–145. https://doi.org/10.1016/j.epsl.2011.12.002

Friedrich, O., Wilson, P. A., Bolton, C. T., Beer, C. J., & Schiebel, R. (2013). Late Pliocene to early Pleistocene changes in the North Atlantic Current and suborbital-scale sea-surface temperature variability. *Paleoceanography*, *28*, 274–282. https://doi.org/10.1002/palo.20029

Grant, K., Grimm, R., Mikolajewicz, U., Marino, G., Ziegler, M., & Rohling, E. (2016). The timing of Mediterranean sapropel deposition relative to insolation, sea-level and African monsoon changes. *Quaternary Science Reviews*, *140*, 125–141. https://doi.org/10.1016/j.quascirev.2016.03.026

Greaves, M., Caillon, N., Rebaubier, H., Bartoli, G., Bohaty, S., Cacho, I., et al. (2008). Interlaboratory comparison study of calibration standards for foraminiferal Mg/Ca thermometry. *Geochemistry, Geophysics, Geosystems*, *9*, Q08010. https://doi.org/10.1029/2008gc001974

Green, D., Cooper, M., German, C., & Wilson, P. (2003). Optimization of an inductively coupled plasma-optical emission spectrometry method for the rapid determination of high-precision Mg/Ca and Sr/Ca in foraminiferal calcite. *Geochemistry, Geophysics, Geosystems*, *4*(6), 8404. https://doi.org/10.1029/2002GC000488

Grousset, F., Labeyrie, L., Sinko, J., Cremer, M., Bond, G., Duprat, J., et al. (1993). Patterns of ice-rafted detritus in the glacial North Atlantic (40–55°N). *Paleoceanography*, *8*, 175–192. https://doi.org/10.1029/92PA02923

Hennissen, J. A., Head, M. J., De Schepper, S., & Groeneveld, J. (2014). Palynological evidence for a southward shift of the North Atlantic Current at ~2.6 Ma during the intensification of Late Cenozoic Northern Hemisphere glaciation. *Paleoceanography*, *29*, 564–580. https://doi.org/10.1002/2013pa002543

Hennissen, J. A., Head, M. J., De Schepper, S., & Groeneveld, J. (2015). Increased seasonality during the intensification of Northern Hemisphere glaciation at the Pliocene–Pleistocene boundary~ 2.6 Ma. *Quaternary Science Reviews*, *129*, 321–332. https://doi.org/10.1016/j.quascirev.2015.10.010

Herbert, T. D., Lawrence, K. T., Tzanova, A., Peterson, L. C., Caballero-Gill, R., & Kelly, C. S. (2016). Late Miocene global cooling and the rise of modern ecosystems. *Nature Geoscience*, *9*(11), 843–847. https://doi.org/10.1038/Ngeo2813

Imbrie, J., Berger, A., Boyle, E. A., Clemens, S. C., Duffy, A., Howard, W. R., et al. (1993). On the structure and origin of major glaciation cycles 1. The 100,000 year cycle. *Paleoceanography*, *8*, 699–735. https://doi.org/10.1029/93PA02751

Imbrie, J., Boyle, E. A., Clemens, S. C., Duffy, A., Howard, W. R., Kukla, G., et al. (1992). On the structure and origin of major glaciation cycles 1. Linear responses to Milankovitch forcing. *Paleoceanography*, *7*, 701–738. https://doi.org/10.1029/92pa02253

Jones, J. I. (1967). Significance of the distribution of planktonic foraminifera in the equatorial Atlantic undercurrent. *Micropaleontology*, *13*(4), 489–501. https://doi.org/10.2307/1484724

Keffer, T. (1985). The ventilation of the world's oceans: Maps of the potential vorticity field. *Journal of Physical Oceanography*, *15*(5), 509–523. https://doi.org/10.1175/1520-0485(1985)015<0509:TVOTWO>2.0.CO;2

Keffer, T., Martinson, D., & Corliss, B. (1988). The position of the Gulf stream during Quaternary glaciations. *Science*, *241*(4864), 440–442. https://doi.org/10.1126/science.241.4864.440

Kemle-von Mücke, S., & Oberhänsli, H. (1999). The distribution of living planktic foraminifera in relation to southeast Atlantic oceanography, in *Use of proxies in paleoceanography*, edited, pp. 91-115, Springer, Berlin, Heidelberg.

Krauss, W. (1986). The North Atlantic current. *Journal of Geophysical Research*, *91*, 5061–5074. https://doi.org/10.1029/JC091iC04p05061

Kuroyanagi, A., & Kawahata, H. (2004). Vertical distribution of living planktonic foraminifera in the seas around Japan. *Marine Micropaleontology*, *53*(1–2), 173–196. https://doi.org/10.1016/j.marmicro.2004.06.001

Lang, D. C., Bailey, I., Wilson, P. A., Beer, C. J., Bolton, C. T., Friedrich, O., et al. (2014). The transition on North America from the warm humid Pliocene to the glaciated Quaternary traced by eolian dust deposition at a benchmark North Atlantic Ocean drill site. *Quaternary Science Reviews*, *93*, 125–141. https://doi.org/10.1016/j.quascirev.2014.04.005

Lang, D. C., Bailey, I., Wilson, P. A., Chalk, T. B., Foster, G. L., & Gutjahr, M. (2016). Incursions of southern-sourced water into the deep North Atlantic during late Pliocene glacial intensification, *Nature Geoscience*, advance online publication. *9*(5), 375–379. https://doi.org/10.1038/ngeo2688

Lawrence, K. T., Herbert, T. D., Brown, C. M., Raymo, M. E., & Haywood, A. M. (2009). High-amplitude variations in North Atlantic Sea surface temperature during the early Pliocene warm period. *Paleoceanography*, *24*, PA2218. https://doi.org/10.1029/2008PA001669

Lawrence, K. T., Sigman, D., Herbert, T., Riihimaki, C., Bolton, C. T., Martinez-Garcia, A., et al. (2013). Time-transgressive North Atlantic productivity changes upon Northern Hemisphere glaciation. *Paleoceanography*, *28*, 740–751. https://doi.org/10.1002/2013PA002546

LeGrande, A. N., & Schmidt, G. A. (2006). Global gridded data set of the oxygen isotopic composition in seawater. *Geophysical Research Letters*, *33*, L12604. https://doi.org/10.1029/2006gl026011

Lisiecki, L. E., & Raymo, M. E. (2005). A Pliocene-Pleistocene stack of 57 globally distributed benthic $\delta^{18}O$ records. *Paleoceanography*, *20*, PA1003. https://doi.org/10.1029/2004PA001071

Locarnini, R. A., Mishonov, A. V., Antonov, J. I., Boyer, T. P., Garcia, H. E., Baranova, O. K., et al. (2013). World Ocean Atlas 2013, Volume 1: Temperature. In S. Levitus (Ed.), *A. Mishonov Technical Ed., NOAA Atlas NESDIS* (Vol. 73, 40 pp.).

Lochte, K., & Pfannkuche, O. (1987). Cyclonic cold-core eddy in the eastern North Atlantic. II. Nutrients, phytoplankton and bacterioplankton. *Marine Ecology Progress Series*, *39*, 153–164. https://doi.org/10.3354/meps039153

Loubere, P. (1988). Gradual late Pliocene onset of glaciation: A deep-sea record from the northeast Atlantic. *Palaeogeography, Palaeoclimatology, Palaeoecology*, *63*(4), 327–334. https://doi.org/10.1016/0031-0182(88)90103-4

Loubere, P., & Moss, K. (1986). Late Pliocene climatic change and the onset of Northern Hemisphere glaciation as recorded in the northeast Atlantic Ocean. *Geological Society of America Bulletin*, *97*(7), 818–828. https://doi.org/10.1130/0016-7606(1986)97<818:Lpccat>2.0.Co;2

Lourens, L. J., Antonarakou, A., Hilgen, F., Van Hoof, A. A. M., Vergnaud-Grazzini, C., & Zachariasse, W. J. (1996). Evaluation of the Plio-Pleistocene astronomical timescale. *Paleoceanography*, *11*, 391–413. https://doi.org/10.1029/96pa01125

Lourens, L. J., Hilgen, F. J., Gudjonsson, L., & Zachariasse, W. J. (1992). Late Pliocene to early Pleistocene astronomically forced sea surface productivity and temperature variations in the Mediterranean. *Marine Micropaleontology*, *19*(1-2), 49–78. https://doi.org/10.1016/0377-8398(92)90021-B

Luyten, J., Pedlosky, J., & Stommel, H. (1983). The ventilated thermocline. *Journal of Physical Oceanography*, *13*(2), 292–309. https://doi.org/10.1175/1520-0485(1983)013<0292:TVT>2.0.CO;2

Marino, G., Rohling, E. J., Rodríguez-Sanz, L., Grant, K. M., Heslop, D., Roberts, A. P., et al. (2015). Bipolar seesaw control on last interglacial sea level. *Nature*, *522*(7555), 197–201. https://doi.org/10.1038/nature14499

McCartney, M. S., & Talley, L. D. (1982). The subpolar mode water of the North Atlantic Ocean. *Journal of Physical Oceanography*, *12*(11), 1169–1188. https://doi.org/10.1175/1520-0485(1982)012<1169:TSMWOT>2.0.CO;2

McIntyre, A., Ruddiman, W., & Jantzen, R. (1972). Southward penetrations of the North Atlantic Polar Front: Faunal and floral evidence of large-scale surface water mass movements over the last 225,000 years, paper presented at Deep Sea Research and Oceanographic Abstracts, Elsevier.

Mittelstaedt, E. (1987). Cyclonic cold-core eddy in the eastern North Atlantic. I. Physical description. *Marine Ecology Progress Series*, *39*, 145–152. https://doi.org/10.3354/meps039145

Moore, M., Mills, M. M., Milne, A., Langlois, R., Achterberg, E. P., Lochte, K., et al. (2006). Iron limits primary productivity during spring bloom development in the central North Atlantic. *Global Change Biology*, *12*(4), 626–634. https://doi.org/10.1111/j.1365-2486.2006.01122.x

Mortyn, P. G., & Charles, C. D. (2003). Planktonic foraminiferal depth habitat and $\delta^{18}O$ calibrations: Plankton tow results from the Atlantic sector of the Southern Ocean. *Paleoceanography*, *18*(2), 1037. https://doi.org/10.1029/2001PA000637

Mudelsee, M., & Raymo, M. E. (2005). Slow dynamics of the Northern Hemisphere glaciation. *Paleoceanography*, *20*, PA4022. https://doi.org/10.1029/2005pa001153

Naafs, B. D. A., Hefter, J., Acton, G., Haug, G. H., Martínez-Garcia, A., Pancost, R., & Stein, R. (2012). Strengthening of North American dust sources during the late Pliocene (2.7 Ma). *Earth and Planetary Science Letters*, *317-318*, 8–19. https://doi.org/10.1016/j.epsl.2011.11.026

Naafs, B. D. A., Hefter, J., Grützner, J., & Stein, R. (2013). Warming of surface waters in the mid-latitude North Atlantic during Heinrich events. *Paleoceanography*, *28*, 153–163. https://doi.org/10.1029/2012PA002354

Naafs, B. D. A., Stein, R., Hefter, J., Khélifi, N., De Schepper, S., & Haug, G. H. (2010). Late Pliocene changes in the North Atlantic current. *Earth and Planetary Science Letters*, *298*(3-4), 434–442. https://doi.org/10.1016/j.epsl.2010.08.023

Oschlies, A., & Garçon, V. (1998). Eddy-induced enhancement of primary production in a model of the North Atlantic Ocean. *Nature*, *394*(6690), 266–269. https://doi.org/10.1038/28373

Pflaumann, U., Sarnthein, M., Chapman, M., d'Abreu, L., Funnell, B., Huels, M., et al. (2003). Glacial North Atlantic: Sea-surface conditions reconstructed by GLAMAP 2000. *Paleoceanography*, *18*(3), 1065. https://doi.org/10.1029/2002PA000774

Poore, R., & Berggren, W. (1975). The morphology and classification of *Neogloboquadrina atlantica* (Berggren). *The Journal of Foraminiferal Research*, *5*(2), 76–84. https://doi.org/10.2113/gsjfr.5.2.76

PRISM Project Members (1996). Pliocene planktic foraminifer census data from the North Atlantic region, U.S. Geological Survey Open File Report(96-669).

Raymo, M. E., Hodell, D., & Jansen, E. (1992). Response of deep ocean circulation to initiation of Northern Hemisphere glaciation (3–2 Ma). *Paleoceanography*, *7*, 645–672. https://doi.org/10.1029/92pa01609

Raymo, M. E., Oppo, D. W., Flower, B. P., Hodell, D. A., McManus, J. F., Venz, K. A., et al. (2004). Stability of North Atlantic water masses in face of pronounced climate variability during the Pleistocene. *Paleoceanography*, *19*, PA2008. https://doi.org/10.1029/2003pa000921

Raymo, M. E., Ruddiman, W. F., Backman, J., Clement, B., & Martinson, D. (1989). Late Pliocene variation in Northern Hemisphere ice sheets and North Atlantic Deep Water circulation. *Paleoceanography*, *4*, 413–446. https://doi.org/10.1029/PA004i004p00413

Raymo, M. E., Ruddiman, W. F., & Clement, B. M. (1986). Pliocene-Pleistocene paleoceanography of the North Atlantic at Deep Sea Drilling Project Site 609. *Deep Sea Drilling Project Initial Reports*, *94*. https://doi.org/10.2973/dsdp.proc.94.125.1987

Raymo, M. E., Ruddiman, W. F., Shackleton, N. J., & Oppo, D. W. (1990). Evolution of Atlantic-Pacific $\delta^{13}C$ gradients over the last 2.5 my. *Earth and Planetary Science Letters*, *97*(3), 353–368.

Regenberg, M., Steph, S., Nürnberg, D., Tiedemann, R., & Garbe-Schönberg, D. (2009). Calibrating Mg/Ca ratios of multiple planktonic foraminiferal species with $\delta^{18}O$-calcification temperatures: Paleothermometry for the upper water column. *Earth and Planetary Science Letters*, *278*(3-4), 324–336. https://doi.org/10.1016/j.epsl.2008.12.019

Regoli, F., Garidel-Thoron, T., Tachikawa, K., Jian, Z., Ye, L., Droxler, A. W., et al. (2015). Progressive shoaling of the equatorial Pacific thermocline over the last eight glacial periods. *Paleoceanography*, *30*, 439–455. https://doi.org/10.1002/2014pa002696

Repschläger, J., Weinelt, M., Kinkel, H., Andersen, N., Garbe-Schönberg, D., & Schwab, C. (2015). Response of the subtropical North Atlantic surface hydrography on deglacial and Holocene AMOC changes. *Paleoceanography*, *30*, 456–476. https://doi.org/10.1002/2014PA002637

Robinson, M. M. (2018). Planktic foraminifer census data for ODP Sites 907, 909 and 911, U.S. Geological Survey data release, doi: https://doi.org/10.5066/P9OFDVZ6.

Robinson, M. M., Dowsett, H. J., Dwyer, G. S., & Lawrence, K. T. (2008). Reevaluation of mid-Pliocene North Atlantic sea surface temperatures. *Paleoceanography*, *23*, PA3213. https://doi.org/10.1029/2008PA001608

Rohling, E. J., Foster, G. L., Grant, K., Marino, G., Roberts, A., Tamisiea, M. E., & Williams, F. (2014). Sea-level and deep-sea-temperature variability over the past 5.3 million years. *Nature*, *508*(7497), 477–482. https://doi.org/10.1038/nature13230

Rohling, E. J., Hayes, A., De Rijk, S., Kroon, D., Zachariasse, W., & Eisma, D. (1998). Abrupt cold spells in the northwest Mediterranean. *Paleoceanography*, *13*, 316–322. https://doi.org/10.1029/98pa00671

Rosenthal, Y., Perron-Cashman, S., Lear, C. H., Bard, E., Barker, S., Billups, K., et al. (2004). Interlaboratory comparison study of Mg/Ca and Sr/Ca measurements in planktonic foraminifera for paleoceanographic research. *Geochemistry, Geophysics, Geosystems*, *5*, Q04D09. https://doi.org/10.1029/2003gc000650

Rossby, T. (1996). The North Atlantic Current and surrounding waters: At the crossroads. *Reviews of Geophysics*, *34*, 463–481. https://doi.org/10.1029/96rg02214

Ruddiman, W. F., & McIntyre, A. (1976). Northeast Atlantic paleoclimatic changes over the past 600,000 years. *Geological Society of America Memoirs*, *145*, 111–146. https://doi.org/10.1130/MEM145-p111

Ruddiman, W. F., McIntyre, A., & Raymo, M. E. (1986). Paleoenvironmental results from North Atlantic sites 607 and 609. *Initial Reports of the Deep Sea Drilling Project*, *94*, 855–878.

Ruddiman, W. F., Raymo, M. E., Martinson, D., Clement, B., & Backman, J. (1989). Pleistocene evolution: Northern Hemisphere ice sheets and North Atlantic Ocean. *Paleoceanography*, *4*, 353–412. https://doi.org/10.1029/PA004i004p00353

Sarmiento, J. (1983). A tritium box model of the North Atlantic thermocline. *Journal of Physical Oceanography*, *13*(7), 1269–1274. https://doi.org/10.1175/1520-0485(1983)013<1269:Atbmot>2.0.Co;2

Sarmiento, J., Gruber, N., Brzezinski, M., & Dunne, J. (2004). High-latitude controls of thermocline nutrients and low latitude biological productivity. *Nature*, *427*(6969), 56–60. https://doi.org/10.1038/nature02127

Schiebel, R., Bijma, J., & Hemleben, C. (1997). Population dynamics of the planktic foraminifer *Globigerina bulloides* from the eastern North Atlantic. *Deep Sea Research Part I: Oceanographic Research Papers*, *44*(9–10), 1701–1713. https://doi.org/10.1016/S0967-0637(97)00036-8

Schiebel, R., & Hemleben, C. (2000). Interannual variability of planktic foraminiferal populations and test flux in the eastern North Atlantic Ocean (JGOFS). *Deep Sea Research Part II: Topical Studies in Oceanography*, *47*(9), 1809–1852. https://doi.org/10.1016/S0967-0645(00)00008-4

Schiebel, R., Hiller, B., & Hemleben, C. (1995). Impacts of storms on recent planktic foraminiferal test production and $CaCO_3$ flux in the North Atlantic at 47 N, 20 W (JGOFS). *Marine Micropaleontology*, *26*(1–4), 115–129. https://doi.org/10.1016/0377-8398(95)00035-6

Schlitzer, R. (2015). Ocean Data View, odv.awi.de, http://odv.awi.de

Schmidt, G. A., & Mulitza, S. (2002). Global calibration of ecological models for planktic foraminifera from coretop carbonate oxygen-18. *Marine Micropaleontology*, *44*(3-4), 125–140. https://doi.org/10.1016/S0377-8398(01)00041-X

Schrag, D. P., Adkins, J. F., McIntyre, K., Alexander, J. L., Hodell, D. A., Charles, C. D., & McManus, J. F. (2002). The oxygen isotopic composition of seawater during the Last Glacial Maximum, *Quaternary Science Reviews*, *21*(1–3), 331–342. https://doi.org/10.1016/S0277-3791(01)00110-X

Shipboard Scientific Party. (2006). Site U1313, edited by J. E. T. Channell, T. Kanamatsu, T. Sato, R. Stein, C. A. Alvarez Zarikian, M. J. Malone and E. Scientists.

Slowey, N. C., & Curry, W. B. (1995). Glacial-interglacial differences in circulation and carbon cycling within the upper western North Atlantic. *Paleoceanography*, *10*, 715–732. https://doi.org/10.1029/95PA01166

Smith, M., Glick, E., Lodestro, S., & Rashid, H. (2013). Data report: Oxygen isotopes and foraminifer abundance record for the last glacial–interglacial cycle and marine isotope stage 6 at IODP Site U1313. *Proceedings of Integrated Ocean Drilling Program*, *303*(306), 306.

Spaak, P. (1982). Accuracy in correlation and ecological aspects of the planktonic foraminiferal zonation of the Mediterranean Pliocene, Utrecht Univ.

Sprintall, J., & Cronin, M. (2001). Upper ocean vertical structure. *Encyclopedia of Ocean Sciences*, *6*, 3120–3129. https://doi.org/10.1006/rwos.2001.0149

Stein, R., Hefter, J., Grützner, J., Voelker, A., & Naafs, B. D. A. (2009). Variability of surface water characteristics and Heinrich-like events in the Pleistocene midlatitude North Atlantic Ocean: Biomarker and XRD records from IODP Site U1313 (MIS 16–9). *Paleoceanography*, *24*, PA2203. https://doi.org/10.1029/2008PA001639

Steph, S., Regenberg, M., Tiedemann, R., Mulitza, S., & Nürnberg, D. (2009). Stable isotopes of planktonic foraminifera from tropical Atlantic/Caribbean core-tops: Implications for reconstructing upper ocean stratification. *Marine Micropaleontology*, *71*(1-2), 1–19. https://doi.org/10.1016/j.marmicro.2008.12.004

Tachikawa, K., Timmermann, A., Vidal, L., Sonzogni, C., & Timm, O. E. (2014). CO_2 radiative forcing and Intertropical Convergence Zone influences on western Pacific warm pool climate over the past 400 ka. *Quaternary Science Reviews*, *86*, 24–34. https://doi.org/10.1016/j.quascirev.2013.12.018

Talley, L. D., Pickard, G. L., Emery, W. J., & Swift, J. H. (2011). Atlantic Ocean, in *Descriptive physical oceanography: An introduction*, 6th ed., edited, pp. 245–301, Academic Press, Cambridge, MA. https://doi.org/10.1016/B978-0-7506-4552-2.10009-5

Tedesco, K., Thunell, R., Astor, Y., & Muller-Karger, F. (2007). The oxygen isotope composition of planktonic foraminifera from the Cariaco Basin, Venezuela: Seasonal and interannual variations. *Marine Micropaleontology*, *62*(3), 180–193. https://doi.org/10.1016/j.marmicro.2006.08.002

The Ring Group. (1981). Gulf stream cold-core rings: Their physics, chemistry, and biology. *Science*, *212*(4499), 1091–1100. https://doi.org/10.1126/science.212.4499.1091

Thirumalai, K., Quinn, T. M., & Marino, G. (2016). Constraining past seawater $\delta^{18}O$ and temperature records developed from foraminiferal geochemistry. *Paleoceanography*, *31*, 1409–1422. https://doi.org/10.1002/2016PA002970

Tolderlund, D. S., & Bé, A. W. H. (1971). Seasonal distribution of planktonic foraminifera in the western North Atlantic. *Micropaleontology*, *17*(3), 297–329. https://doi.org/10.2307/1485143

Trossman, D., Thompson, L., Mecking, S., & Warner, M. (2012). On the formation, ventilation, and erosion of mode waters in the North Atlantic and southern oceans. *Journal of Geophysical Research*, *117*, C09026. https://doi.org/10.1029/2012jc008090

Versteegh, G. J., Brinkhuis, H., Visscher, H., & Zonneveld, K. A. (1996). The relation between productivity and temperature in the Pliocene North Atlantic at the onset of Northern Hemisphere glaciation: A palynological study. *Global and Planetary Change*, *11*(4), 155–165. https://doi.org/10.1016/0921-8181(95)00054-2

Vidal, L., Labeyrie, L., Cortijo, E., Arnold, M., Duplessy, J., Michel, E., et al. (1997). Evidence for changes in the North Atlantic Deep Water linked to meltwater surges during the Heinrich events. *Earth and Planetary Science Letters*, *146*(1-2), 13–27. https://doi.org/10.1016/S0012-821X(96)00192-6

Villanueva, J., Calvo, E., Pelejero, C., Grimalt, J., Boelaert, A., & Labeyrie, L. (2001). A latitudinal productivity band in the central North Atlantic over the last 270 kyr: An alkenone perspective. *Paleoceanography*, *16*, 617–626. https://doi.org/10.1029/2000PA000543

Villanueva, J., Grimalt, J. O., Cortijo, E., Vidal, L., & Labeyrie, L. (1998). Assessment of sea surface temperature variations in the central North Atlantic using the alkenone unsaturation index (U 37 K′). *Geochimica et Cosmochimica Acta*, *62*(14), 2421–2427. https://doi.org/10.1016/S0016-7037(98)00180-X

Villanueva, J., Grimalt, J. O., Labeyrie, L. D., Cortijo, E., Vidal, L., & Louis-Turon, J. (1998). Precessional forcing of productivity in the North Atlantic Ocean. *Paleoceanography*, *13*, 561–571. https://doi.org/10.1029/98PA02318

Waelbroeck, C., Paul, A., Kucera, M., Rosell-Melé, A., Weinelt, M., Schneider, R., et al. (2009). Constraints on the magnitude and patterns of ocean cooling at the Last Glacial Maximum. *Nature Geoscience*, *2*(2), 127–132. https://doi.org/10.1038/Ngeo411

Wang, L. (2000). Isotopic signals in two morphotypes of *Globigerinoides ruber* (white) from the South China Sea: Implications for monsoon climate change during the last glacial cycle. *Palaeogeography, Palaeoclimatology, Palaeoecology*, *161*(3-4), 381–394. https://doi.org/10.1016/S0031-0182(00)00094-8

Wang, P., Tian, J., & Lourens, L. J. (2010). Obscuring of long eccentricity cyclicity in Pleistocene oceanic carbon isotope records. *Earth and Planetary Science Letters*, *290*(3-4), 319–330. https://doi.org/10.1016/j.epsl.2009.12.028

Zachariasse, W., Gudjonsson, L., Hilgen, F., Langereis, C., Lourens, L., Verhallen, P., & Zijderveld, J. (1990). Late Gauss to early Matuyama invasions of *Neogloboquadrina atlantica* in the Mediterranean and associated record of climatic change. *Paleoceanography*, *5*, 239–252. https://doi.org/10.1029/PA005i002p00239